Distinct C−H Bond Activation Pathways in Diamido-Pyridine-Supported Rare-Earth Metal Hydrocarbyl Complexes

Melanie Zimmermann,[†] Frank Estler,[‡] Eberhardt Herdtweck,[‡] Karl W. Törnroos,[†] and Reiner Anwander*,[†]

Department of Chemistry, University of Bergen, Allégaten 41, N-5007, Bergen, Norway, and Department Chemie, Lehrstuhl für Anorganische Chemie, Technische Universität München, Lichtenbergstrasse 4, D-85747 Garching bei München, Germany

Received August 14, 2007

Transition metal precatalyst−organoaluminum cocatalyst interactions are of fundamental importance in Ziegler−Natta polymerization catalysis. Rare-earth metal tetramethylaluminate complexes (BDPPpyr)Ln($AlMe_4$) bearing a [**N**N**N**]$^{2-}$ post-metallocene-type ligand (H_2BDPPpyr = 2,6-bis-(((2,6-diisopropylphenyl)amino)methyl)pyridine) were obtained by two different synthesis routes. Reaction of (BDPPpyr)Ln(NEt_2)(THF) with trimethylaluminum afforded complexes (BDPPpyr)Ln($AlMe_4$) of the small rare-earth metals scandium and lutetium. Corresponding compounds of the larger metals yttrium and lanthanum were synthesized according to the tetramethylaluminate route, i.e., the reaction of Ln($AlMe_4$)$_3$ with H_2-BDPPpyr produced (BDPPpyr)Ln($AlMe_4$), along with the byproduct (BDPPpyr)($AlMe_2$)$_2$. Dynamic NMR spectroscopy of (BDPPpyr)Ln($AlMe_4$) revealed distinct fluxional behavior of the $AlMe_4^-$ ligand depending on the metal size (Lu: *associative* via Lu(μ-Me)$_3$AlMe; Sc: *dissociative* via Sc(μ-Me)$AlMe_3$). In the presence of trimethylaluminum, the yttrium derivative undergoes a ligand backbone metalation at the isopropyl methyl group yielding (BDPPpyr-**H**)Y[(μ-Me)$AlMe_2$]$_2$ featuring a [**N**N**NC**]$^{3-}$-type ligand. For the lutetium derivative, addition of THF caused cyclometallation products (BDPPpyr-**H**)Lu[(μ-Me)$AlMe_2$]-(THF) and [Lu(BDPPpyr-**H**)]$_2$ involving the isopropyl methine proton. Present studies not only clearly show the enhanced reactivity of rare-earth metal methyl moieties [Ln−Me] but also that excessive use of organoaluminum cocatalysts can result in gradual ligand degradation and concomitant catalyst deactivation. The findings might contribute to a better understanding of activation/deactiviation sequences in post-metallocene-promoted olefin polymerization.

Introduction

Ancillary ligand design and metal cationization (= generation of highly electron-deficient metal centers) are most prolific strategies for improving the overall performance of homogeneous polymerization catalysts.[1] The challenge of optimizing the catalyst efficiency, however, often turns into a tightrope walk between ultimate activity (and selectivity) and catalyst deactivation as evidenced by solvent attack and/or self-degradation.[2] The latter is clearly manifested by (a) (multiple) hydrogen abstraction occurring in metal-bonded alkyl ligands (e.g., alkylidene formation in *Tebbe*-analogous reagents) accompanied by metal complex clustering[3] and (b) ancillary ligand derivatization via inter- and intramolecular C−H bond activation.[4−13] Early transition metal alkyl and hydride complexes [(Cp′)$_2$MR_x]$_y$ (Cp′ = substituted cyclopentadienyl, R = alkyl, hydride)

* Corresponding Author. Prof. Dr. Reiner Anwander, Department of Chemistry, University of Bergen, Allégaten 41, N-5007, Bergen, Norway. E-mail: Reiner.Anwander@kj.uib.no. Tel.: +47 555 89491. Fax: +47 555 89490.

[†] University of Bergen.

[‡] Technische Universität München.

(1) (a) Brintzinger, H. H.; Fischer, D.; Mühlhaupt, R.; Rieger, B.; Waymouth, R. M. *Angew. Chem., Int. Ed. Engl.* **1995**, *34*, 1143. (b) McKnight, A. L.; Waymouth, R. M. *Chem. Rev.* **1998**, *98*, 2587. (c) Alt, H. G.; Köppl, A. *Chem. Rev.* **2000**, *100*, 1205. (d) Hou, Z.; Wakatsuki, Y. *Coord. Chem. Rev.* **2002**, *231*, 1. (e) Gromada, J.; Carpentier, J. F.; Mortreux, A. *Coord. Chem. Rev.* **2004**, *248*, 397. (f) Bochmann, M. *J. Organomet. Chem.* **2004**, *689*, 3982. (g) Hyeon, J. Y.; Gottfriedsen, J.; Edelmann, F. T. *Coord. Chem. Rev.* **2005**, *249*, 2787. (h) Zeimentz, P. M.; Arndt, S.; Elvidge, B. R.; Okuda. J. *Chem. Rev.* **2006**, *106*, 2404, and references therein.

(2) (a) Thompson, M. E.; Baxter, S. M.; Bulls, A. R.; Burger, B. J.; Nolan, M. C.; Santarsiero, B. D.; Schaefer, W. P.; Bercaw, J. E. *J. Am. Chem. Soc.* **1987**, *109*, 203. (b) Ma, K.; Piers, W. E.; Parvez, M. *J. Am. Chem. Soc.* **2006**, *128*, 3303. (c) Jantunen, K. C.; Scott, B. L.; Gordon, J. L.; Kiplinger, J. L. *Organometallics* **2007**, *26*, 2777.

(3) (a) Guérin, F.; Stephan, D. *Angew. Chem., Int. Ed.* **1999**, *38*, 3698. (b) Kickham, J. E.; Guérin, F.; Stewart, J. C.; Stephan, D. *Angew. Chem., Int. Ed.* **2000**, *39*, 3263. (c) Kickham, J. E.; Guérin, F.; Stewart, J. C.; Urbanska, E.; Stephan, D. *Organometallics* **2001**, *20*, 1175. (d) Yue, N.; Hollink, E.; Guérin, F.; Stephan, D. *Organometallics* **2001**, *20*, 4424. (e) Kickham, J. E.; Guérin, F.; Stephan, D. *J. Am. Chem. Soc.* **2002**, *124*, 11486. (f) Stephan, D. *Organometallics* **2005**, *24*, 2548.

(4) (a) Watson, P. L.; Parshall, G. W. *Acc. Chem. Res.* **1985**, *18*, 51. (b) Thompson, M. E.; Bercaw, J. E. *J. Pure Appl. Chem.* **1984**, *56*, 1. (c) Watson, P. L. *J. Chem. Soc., Chem. Commun.* **1983**, 276. (d) Watson, P. L. *J. Am. Chem. Soc.* **1983**, *105*, 6491. (d) Booij, M.; Deelman, B.-J.; Duchateau, R.; Postma, D. S.; Meetsma, A.; Teuben, J. H. *Organometallics* **1993**, *12*, 3531. (e) Deelman, B.-J.; Teuben, J. H.; MacGregor, S. A.; Eisenstein, O. *New J. Chem.* **1995**, *19*, 691. (f) Sadow, A. D.; Tilley, T. D. *J. Am. Chem. Soc.* **2003**, *125*, 7971. (g) Evans, W. J.; Chamberlain, L. R.; Ulibarri, T. A.; Ziller, J. W. *J. Am. Chem. Soc.* **1988**, *110*, 6423. (h) Evans, W. J.; Ulibarri, T. A.; Ziller, J. W. *Organometallics* **1991**, *10*, 134. (i) Evans, W. J.; Perotti, J. M.; Ziller, J. W. *J. Am. Chem. Soc.* **2005**, *127*, 1068. (j) Evans, W. J.; Perotti, J. M.; Ziller, J. W. *J. Am. Chem. Soc.* **2005**, *127*, 3894. (k) Sadow, A. D.; Tilley, T. D. *J. Am. Chem. Soc.* **2005**, *127*, 643. (l) Booij, M.; Meetsma, A.; Teuben, J. H. *Organometallics* **1991**, *10*, 3246. (m) Evans, W. J.; Perotti, J. M.; Ziller, J. W. *Inorg. Chem.* **2005**, *44*, 5820. (n) Evans, W. J.; Champagne, T. M.; Ziller, J. W. *J. Am. Chem. Soc.* **2006**, *128*, 14270. (o) Woodrum, N. L.; Cramer, C. J. *Organometallics* **2006**, *25*, 68. (p) Lewin, J. L.; Woodrum, N. L.; Cramer, C. J. *Organometallics* **2006**, *25*, 5906.

10.1021/om700830k CCC: $37.00
Publication on Web 10/23/2007

Chart 1

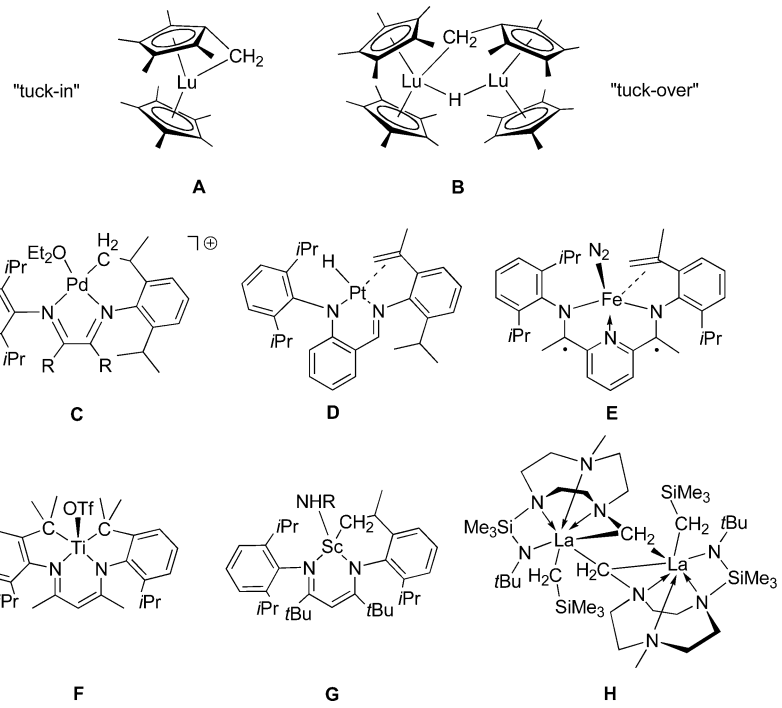

carrying the ubiquitous and robust/rigid cyclopentadienyl ancillary ligand display exceptional potential in the stereoselective polymerization of olefins.[1] The cyclopentadienyl ligand implies highly electron-deficient metal centers facilitating C−H bond activation of the polymer alkyl ligand which either assists (α-agostic interaction) or terminates (*β*-agostic interaction → *β*-H elimination) chain growth. In addition, intramolecular C−H activation or cyclometallation involving the ancillary ligand backbone is a commonly observed "deactivation" reaction among early transition metal complexes. "Tuck-in" (Chart 1, **A**) and "tuck-over" complexes (Chart 1, **B**) are prominent examples of characteristic C−H bond metalation processes, well documented for rare-earth,[4b,d,f,h,k−p] group 4,[2a,5] and group 5[6] metallocene complexes. Hence, C−H bond activation is a key feature for the mechanistic understanding of chain termination and catalyst deactivation products in *Ziegler-Natta* polymerization.

During the past 15 years new non-metallocene catalyst families (post-metallocenes), mainly based on functionalized chelating nitrogen (imines, amides) and oxygen donor ligands (alkoxides) have evolved and attracted considerable attention in the field of polymer science.[14] Crucially, C−H bond activation pathways seem to be as persistent as for metallocene complexes, whereas C−H bond cleavage can proceed via oxidative addition to an electron-rich and coordinatively unsaturated late transition metal center or via *σ*-bond metathesis at highly electron-deficient early transition metals. Aside from mechanistic details, the formation of cyclometallation products is a repetitive pattern in post-metallocene chemistry across the entire transition metal series (Chart 1, **C**−**H**).[7−11,13] It clearly reflects the ambivalence of very reactive organometallics acting as high-performance catalysts and concurrently favoring catalyst decomposition pathways.

Pyridine diamido ligands of the [**N**N**N**]$^{2-}$ divalent type as introduced by *McConville* et al. represent archetypal alternative ligand systems to successfully mimic the stereoelectronic features and polymerization behavior of metallocene complexes of Ti(IV),[15] Zr(IV),[16] and Ta(V).[17] This dianionic tridentate ancillary ligand coordinates exclusively in a meridional fashion to the metal center and provides an extremely rigid and planar

(5) (a) Bercaw, J. E.; Marvich, R. H.; Bell, L. G.; Brintzinger, H.-H. *J. Am. Chem. Soc.* **1972**, *94*, 1219. (b) Pattiasina, J. W.; Hissink, C. E.; de Boer, J. L.; Meetsma, A.; Teuben, J. H. *J. Am. Chem. Soc.* **1985**, *107*, 7758. (c) Bulls, A. R.; Schaefer, W. P.; Serfas, M.; Bercaw, J. E. *Organometallics* **1987**, *6*, 1219. (d) Schock, L. E.; Brock, C. P.; Marks, T. J. *Organometallics* **1987**, *6*, 232. (e) Tjaden, E. B.; Stryker, J. M. *J. Am. Chem. Soc.* **1993**, *115*, 2083. (f) Sun, Y.; Spence, R. E. v. H.; Piers, W. E.; Parvez, M.; Yap, G. P. A. *J. Am. Chem. Soc.* **1997**, *119*, 5132. (g) Pool, J. A.; Bradley, C. A.; Chirik, P. J. *Organometallics* **2002**, *21*, 1271. (h) Bernskoetter, W. H.; Pool, J. A.; Lobkovsky, E.; Chirik, P. J. *Organometallics* **2006**, *25*, 1092.

(6) Riley, P. N.; Parker, J. R.; Fanwick, P. E.; Rothwell, I. P. *Organometallics* **1999**, *18*, 3579.

(7) Tempel, D. J.; Johnson, L. K.; Huff, R. L.; White, P. S.; Brookhart, M. *J. Am. Chem. Soc.* **2000**, *122*, 6686.

(8) Kloek, S. M.; Goldberg, K. I. *J. Am. Chem. Soc.* **2007**, *129*, 3460.

(9) Basuli, F.; Bailey, B. C.; Watson, L. A.; Tomaszewski, J.; Huffman, J. C.; Mindiola, D. J. *Organometallics* **2005**, *24*, 1886.

(10) Bart, S. C.; Bowman, A. C.; Lobkovsky, E.; Chirik, P. J. *J. Am. Chem. Soc.* **2007**, *129*, 7212.

(11) (a) Knight, L. K.; Piers, W. E.; Fleurat-Lessard, P.; Parvez, M.; McDonald, R. *Organometallics* **2004**, *23*, 2087. (b) Knight, L. K.; Piers, W. E.; McDonald, R. *Organometallics* **2006**, *25*, 3289.

(12) Bambirra, S.; Boot, S. J.; van Leusen, D.; Meetsma, A.; Hessen, B. *Organometallics* **2004**, *23*, 1891.

(13) Tazelaar, C. G. J.; Bambirra, S.; van Leusen, D.; Meetsma, A.; Hessen, B.; Teuben, J. H. *Organometallics* **2004**, *23*, 936.

(14) For Reviews see: (a) Britovsek, G. J. P.; Gibson, V. C.; Wass, D. F. *Angew. Chem., Int. Ed.* **1999**, *38*, 428. (b) Kempe, R. *Angew. Chem., Int. Ed.* **2000**, *39*, 468. (c) Gade, L. H. *Acc. Chem. Res.* **2002**, *35*, 575. (d) Piers, W. E.; Emslie, D. J. H. *Coord. Chem. Rev.* **2002**, *233*−*234*, 131. (e) Gibson, V. C.; Spitzmesser, S. K. *Chem. Rev.* **2003**, *103*, 283.

(15) (a) Guérin, F.; McConville, D. H.; Payne, N. C. *Organometallics* **1996**, *15*, 5085. (b) Guérin, F.; McConville, D. H.; Vittal, J. J. *Organometallics* **1997**, *16*, 1491. (BDPPpyr)Ti([C_4H_2(SiMe_3)$_2$]: N1-Ti1−N2 141.5(3)°.

(16) (a) Guérin, F.; McConville, D. H.; Vittal, J. J. *Organometallics* **1996**, *15*, 5586. (b) Guérin, F.; McConville, D. H.; Vittal, J. J.; Yap, G. A. P. *Organometallics* **1998**, *17*, 5172. (c) Guérin, F.; Del Vecchio, O.; McConville, D. H. *Polyhedron* **1998**, *17*, 917. (BDPPpyr)Zr(C_4H_6): N2−Zr−N2A 140.0(4)°.

(17) (a) Guérin, F.; McConville, D. H.; Vittal, J. J. *Organometallics* **1995**, *14*, 3154. (b) Guérin, F.; McConville, D. H.; Vittal, J. J.; Yap, G. A. P. *Organometallics* **1998**, *17*, 1290. (BDPPpyr)Ta(η^2-PrC≡CPr)Cl: N1−Ta1−N3 137.2(2)°.

Scheme 1. Reaction of (BDPPpyr)Ln(NEt$_2$)(THF) (2) with AlMe$_3$

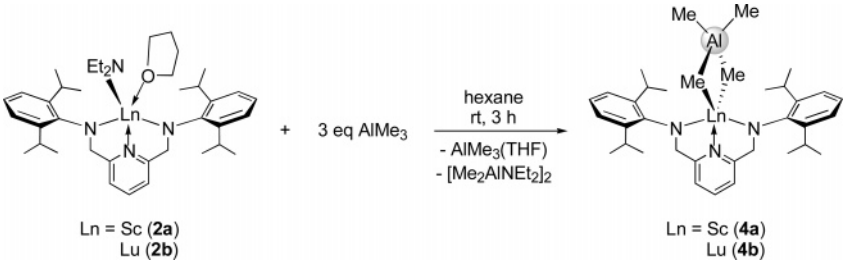

environment. It further proved suitable for accommodating a wide size range of metal centers.[15−19] The catalytic performance of group 4 complexes supported by pyridine diamido ligands, however, exhibited extreme sensitivity toward the choice of the metal center. Whereas (BDPPpyr)$ZrCl_2$ (H_2BDPPpyr = 2,6-bis-(((2,6-diisopropylphenyl)amino)methyl)pyridine) revealed to be a highly active polymerization initiator upon activation with methylaluminoxane (MAO),[16a] the corresponding Ti(IV) compound showed only very low activities toward ethylene.[15a] Catalyst deactivation, due to reduction to Ti(III), was presumed, but interaction of the MAO cocatalyst with the pyridine diamido complex could imply further deactivation pathways. For MAO-activated initiators (typically containing up to 15 wt % $AlMe_3$), cationic bimetallic species $[LM(\mu\text{-}R)_2AlR_2]^+$ are discussed as catalyst resting states ("dormant species").[1a,1f,20] Moreover, these species are important intermediates in chain transfer and catalyst deactivation processes.[20] Although such bimetallic group 4 cations have been studied spectroscopically and computationally, it was only recently that *Mountford* et al. reported the first example of a structurally authenticated group 4 tetramethylaluminate [Ti(N*t*Bu)(Me_3[9]aneN_3)(μ-Me)$_2$$AlMe_2$][B($C_6F_5$)$_4$].[21] Nevertheless, group 4 metallocene and post-metallocene systems often produce intricate catalyst mixtures hampering closer investigations of active species, initiation, propagation as well as catalyst deactivation pathways.[22] Given the intrinsic interrelation between group 4 and group 3/lanthanide metal polymerization chemistry, lanthanide complexes proved to be ideal model systems for *Ziegler* catalysts. Fundamental studies on the interaction of rare-earth metallocene hydrocarbyl derivatives with α-olefins by Watson[4a,23] and Bercaw[24] marked a major breakthrough to understanding mechanistic and kinetic details of olefin insertion and termination processes such as β-H elimination, β-alkyl elimination, or C−H bond activation ("lanthanide model" of Ziegler−Natta polymerization).

Our recent work in the field of heterobimetallic Ln/Al complexes emphasizes the suitability of homoleptic lanthanide tetramethylaluminates Ln($AlMe_4$)$_3$ to act as convenient syntheses precursors,[25] offering straightforward entry into **donor solvent-free** half-lanthanidocene,[26] lanthanidocene,[27] and post-lanthanidocene chemistry.[28,29] In this context, we reported the syntheses of lanthanide tetramethylaluminate complexes bearing [**N**O**N**]$^{2-}$ and [**NNN**]$^{2-}$ type ancillary ligands. Herein we extend this "tetramethylaluminate route" to the pyridine diamido ligand (BDPPpyr), which we previously used in the synthesis of distinct and stable Ln(III) complexes.[18] Besides solid-state structural features, special emphasis is put on the dynamic behavior of the resulting post-lanthanidocene complexes in solution. Furthermore, we account in detail on the complex stability considering the size of the central lanthanide cation and the composition of the reaction mixtures. Finally, C−H bond activation via σ-bond metathesis is discussed as a possible deactivation pathway in group 3 (lanthanide)/group 4 post-metallocene catalyzed olefin polymerization.

Results and Discussion

Synthesis and Structural Features of (BDPPpyr)Ln(AlMe$_4$) Complexes. Trimethylaluminum promoted alkylation of lanthanide amide compounds has been found to be a viable route for the synthesis of donor solvent-free rare-earth metal tetramethylaluminates, that is, rare-earth metal hydrocarbyl complexes. Since the first proof of a $AlMe_3$ mediated complete [NR_2] → [$AlMe_4$] transformation,[30] several publications documented the universal applicability of this synthesis route.[31−33] A high yield synthesis of lanthanide tetramethylaluminates though is governed by steric restrictions and the choice of monoanionic lanthanide amide precursors is often limited to small amide functionalities (NMe_2, NEt_2). Treatment of (BDPPpyr)Ln(NEt_2)(THF) (Ln = Sc (**2a**), Lu (**2b**)) with 3 eq of $AlMe_3$ in hexane afforded the tetramethylaluminate complexes (BDPPpyr)Sc($AlMe_4$) (**4a**) and (BDPPpyr)Lu($AlMe_4$) (**4b**) in almost quantitative yields (Scheme 1). The volatility of

(18) Estler, F.; Eickerling, G.; Herdtweck, E.; Anwander, R. *Organometallics* **2003**, *22*, 1212. (BDPPpyr)Sc(CH_2SiMe_3)(THF): N1−Sc−N2 137.04(6)°.

(19) Cruz, C. A.; Emslie, D. J. H.; Harrington, L. E.; Britten, J. F.; Robertson, C. M. *Organometallics* **2007**, *26*, 692. (BDPPpyr)$ThCl_2$(dme): N1−Th1−N3 128.08°.

(20) (a) Bochmann, M.; Lancaster, S. J. *Angew. Chem., Int. Ed. Engl.* **1994**, *33*, 1634. (b) Britovsek, P.; Cohen, S. A.; Gibson, V. C.; van Meurs, M. *J. Am. Chem. Soc.* **2004**, *126*, 10701. (c) Petros, R. A.; Norton, J. R. *Organometallics* **2004**, *23*, 5105. (d) Lyakin, O. Y.; Bryliakov, K. P.; Semikolenova, N. M.; Lebedev, A. Y.; Voskoboynikov, A. Z.; Zakharov, V. A.; Talsi, E. P. *Organometallics* **2007**, *26*, 1536.

(21) Bolton, P. D.; Clot, E.; Cowley, A. R.; Mountford, P. *Chem. Commun.* **2005**, 3313.

(22) Thiele, H.-K.; Wilson, D. R. *J. Macromol. Sci., Polym. Rev.* **2003**, *C43*, 581.

(23) (a) Watson, P. L. *J. Am. Chem. Soc.* **1982**, *104*, 337. (b) Watson, P. L.; Roe, D. C. *J. Am. Chem. Soc.* **1982**, *104*, 6471.

(24) (a) Burger, B. J.; Thompson, M. E.; Cotter, W. D.; Bercaw, J. E. *J. Am. Chem. Soc.* **1990**, *112*, 1566. (b) Piers, W. E.; Bercaw, J. E. *J. Am. Chem. Soc.* **1990**, *112*, 9406. (c) Burger, B. J.; Cotter, W. D.; Coughlin, E. B.; Chacon, S. T.; Hajela, S.; Herzog, T. A.; Köhn, R.; Mitchell, J.; Piers, W. E.; Shapiro, P. J.; Bercaw, J. E. In *Ziegler Catalysts*; Fink, G., Mühlhaupt R., Brintzinger, H.-H., Eds.; Springer-Verlag: Berlin, 1995; pp 317−331.

(25) Fischbach, A.; Anwander, R. *Adv. Polym. Sci.* **2006**, *204*, 155.

(26) Dietrich, H. M.; Zapilko, C.; Herdtweck, E.; Anwander, R. *Organometallics* **2005**, *24*, 5767.

(27) Zimmermann, M.; Dietrich, H. M.; Anwander, R. Unpublished results.

(28) Zimmermann, M.; Törnroos, K. W.; Anwander, R. *Organometallics* **2006**, *25*, 3593.

(29) Zimmermann, M.; Törnroos, K. W.; Anwander, R. *Angew. Chem., Int. Ed.* **2007**, *46*, 3126.

(30) Evans, W. J.; Anwander, R.; Ziller, J. W. *Organometallics* **1995**, *14*, 1107.

(31) Anwander, R.; Klimpel, M. G.; Dietrich, H. M.; Shorokhov, D. J.; Scherer, W. *Chem. Commun.* **2003**, 1008.

(32) Klimpel, M. G.; Anwander, R.; Tafipolsky M.; Scherer, W. *Organometallics* **2001**, *20*, 3983.

(33) Zimmermann, M.; Frøystein, N. Å.; Fischbach. A.; Sirsch, P.; Dietrich, H. M.; Törnroos, K. W.; Herdtweck, E.; Anwander, R. *Chem.−Eur. J.* **2007**, DOI: 10.1002/chem.200700534.

Scheme 2. Reaction of H_2BDPPpyr (H_2[1]) with Ln(AlMe$_4$)$_3$ (3)

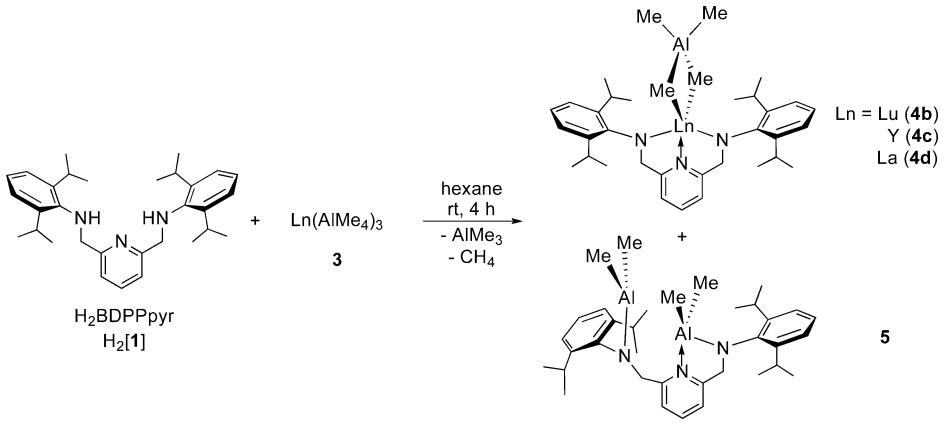

the byproducts, organoaluminum amide $[Me_2AlNEt_2]_2$ and THF adduct $AlMe_3$(THF), allows for an easy separation from complexes **4** (CAUTION: volatiles containing trimethylaluminum react violently when exposed to air). Attempts to synthesize compounds **4a** and **4b** by alkylation of the respective bis(dimethylsilyl)amido or diisopropylamido compounds failed—probably due to effective steric shielding of the (silyl)amide ligands.

Whereas alkylation of the lanthanide amide complexes follows a straightforward high yield synthesis protocol, starting compounds (BDPPpyr)Ln(NEt_2)(THF) (**2**) can only be obtained by a two-step reaction sequence from $Ln(CH_2SiMe_3)_3(THF)_x$ in moderate yields.[18] It is further limited to small to medium sized lanthanide metal centers.[34] To access the entire size range of Ln^{3+} cations, homoleptic lanthanide tetramethylaluminates Ln(AlMe$_4$)$_3$ (**3**) were employed as alkyl precursors. Ln(AlMe$_4$)$_3$ (Ln = Lu (**3b**), Y (**3c**), and La (**3d**)) react with H_2BDPPpyr (H_2[**1**]) according to an alkane elimination reaction to yield the desired complexes (BDPPpyr)Ln(AlMe$_4$) (**4**) in a one-step synthesis (Scheme 2).

Instant gas evolution and precipitation of white solid material evidenced coordination of the diamido ligand to the metal center. Separation of the precipitate from the reaction mixture afforded off-white powdery complexes **4b**, **4c**, and **4d** with yields increasing according to the size of the metal cation (Ln = Lu, 73%; Y, 75%; La, 81%). Colorless single crystals of **4b** suitable for X-ray diffraction analysis were grown from hexane solution and revealed the anticipated formation of (BDPPpyr)Lu(AlMe$_4$) (**4b**) (Figure 1).[35] The five-coordinate Lu center is surrounded by three nitrogen atoms of the BDPPpyr ancillary ligand and two methyl carbons of the η^2-coordinated tetramethylaluminate moiety. The coordination geometry of the lutetium center is best described as distorted trigonal bipyramidal with the amido nitrogen atoms (N2 and N2′) and a tetramethylaluminate carbon (C2) forming the equatorial plane. The pyridine nitrogen N1 and the second tetramethylaluminate carbon C1 occupy the apical positions (N1−Lu−C1, 150.3(1)°). The approximately planar BDPPpyr ligand coordinates in a meridional fashion to the metal center, the ligand bite angle (138.6(1)°) being similar to those reported for Sc,[18] Th,[19] Ti(IV),[15] Zr(IV),[16] and Ta(V)[17] complexes supported by this pincer ligand. Strong interaction of the [**N**N**N**]$^{2-}$ ligand with the central metal is substantiated by a Lu−N2 bond length of 2.186(2) Å. For comparison, the Lu−N bond distances in five-coordinate lutetium amide complex $Lu[N(SiHMe_2)_2]_3(THF)_2$ are 2.184(3), 2.238(3), and 2.253(3) Å).[36] The aryl rings lie perpendicular to the plane of the ligand with an interplanar angle of 82.50(5)°, in a way that the aryl isopropyl groups protect the metal above and below the N_3 plane. Two methyl groups of the [AlMe$_4$] unit coordinate to the central Lu metal in a classical η^2 fashion forming a planar [Ln(μ-CH$_3$)$_2$Al] heterocycle (torsion angles Lu−C1−Al1−C2, C1−Al1−C2−Lu = 0.00°). The Lu−C1 (2.424(3) Å) and Lu−C2 (2.435(3) Å) bond lengths are comparatively short (Cp*Lu(AlMe$_4$)$_2$, 2.501(3)−2.597(3) Å)[31] and the consequent short Lu−H distances of an average 2.29(2) Å implicate intramolecular contacts of two of the three H atoms in each bridging methyl group with the sterically unsaturated and Lewis acidic lutetium metal center.

The ^{1}H NMR spectra of complexes **4** in C_6D_6 are consistent with a rigid meridional coordination of the BDPPpyr ligand to the metal center. The singlet observed for the *N*-methylene protons (4.72 (**4a**), 4.92 (**4b**), 4.80 (**4c**), and 4.99 ppm (**4d**)) as well as only one observed multiplet for the methine groups (3.42 (**4a**), 3.53 (**4b**), 3.43 (**4c**), and 3.20 ppm (**4d**)) are indicative of a highly symmetric environment at the lanthanide metal center. The diastereotopic isopropyl methyl groups show two doublets due to restricted rotation of the aryl groups around the N−C$_{ipso}$ bond. For the lutetium, yttrium, and lanthanum complexes (**4b**−**d**) the ^{1}H NMR spectrum shows only one signal in the methyl alkyl region at −0.33 (**4b**), −0.53 (**4c**), and −0.46 ppm (**4d**), respectively, which can be assigned to the [Al(μ-Me)$_2$Me$_2$] moieties indicating a rapid exchange of bridging and terminal methyl groups. These resonances are shifted to higher field compared to the homoleptic precursors (−0.09, **3b**; −0.25, **3c**; −0.27 ppm, **3d**). A signal splitting of the ^{1}H methyl resonance in **4c** is clearly attributable to a ^{1}H−^{89}Y scalar coupling ($^2J_{YH}$ = 3 Hz).[37] Interestingly, the ^{1}H NMR spectrum as well as the ^{13}C NMR spectrum of the scandium derivative **4a** revealed two different signals for the bridging (^{1}H, 0.35 ppm; ^{13}C, 16.5 ppm) and the terminal methyl groups (^{1}H, −1.11 ppm; ^{13}C, −9.1 ppm) of the [AlMe$_4$] ligand. Apparently, steric hindrance at the smallest rare-earth metal center scandium results in a significantly lower rate of the methyl group exchange.

(34) (a) Lappert, M. F.; Pearce, R. *J. Chem. Soc., Chem. Commun.* **1973**, 126. (b) Atwood, J. L.; Hunter, W. E.; Rogers, R. D.; Holton, J.; McMeeking, J.; Pearce, R.; Lappert, M. F. *J. Chem. Soc., Chem. Commun.* **1978**, 140. (c) Schumann, H.; Müller, J. *J. Organomet. Chem.* **1978**, *146*, C5. (d) Schumann, H; Freckmann, D. M. M.; Dechert, S. *Z. Anorg. Allg. Chem.* **2002**, *628*, 2422. (e) Niemeyer, M. *Acta Crystallogr.* **2001**, *E57*, m553.

(35) Compound **4b** crystallizes from toluene in the triclinic space group *P*1 with a = 13.0374(1) Å, b = 13.6550(1) Å, c = 13.8172(1) Å, α = 86.6742(3)°, β = 69.2809(3)°, γ = 74.5579(2)°.

(36) Anwander, R.; Runte, O.; Eppinger, J.; Gerstberger, G.; Herdtweck, E.; Spiegler, M. *J. Chem. Soc., Dalton Trans.* **1998**, 847.

(37) Such signal splitting was also found for Y(AlMe$_4$)$_3$ (**3c**) at temperatures well above coalescence (ref 33).

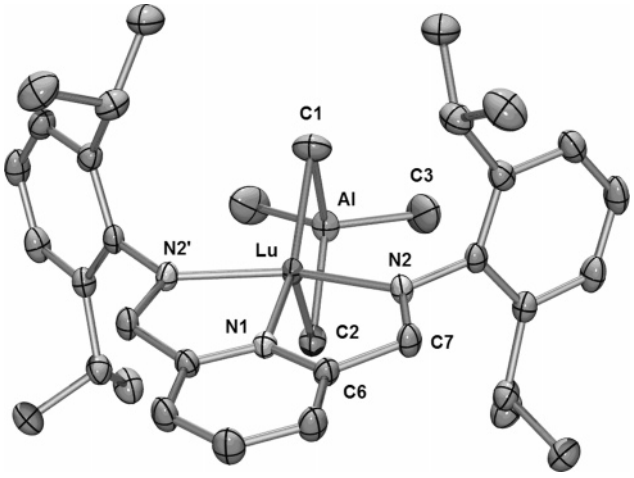

Figure 1. Molecular structure of (BDPPpyr)Lu($AlMe_4$) (**4b**) (atomic displacement parameters set at the 50% level). Hydrogen atoms and the solvent molecule are omitted for clarity.

Scheme 3. Dissociative versus Associative Methyl Group Exchange in (BDPPpyr)Ln[(μ-Me)$_2$AlMe$_2$] (4)

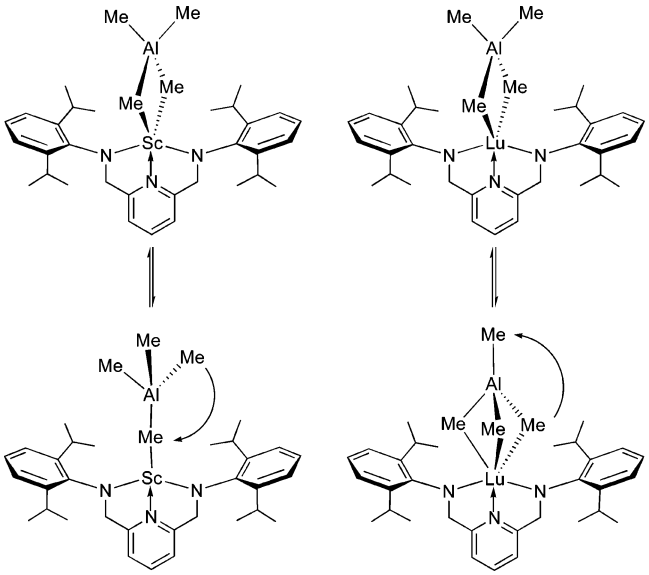

Hence, two separate signals for the different methyl groups of the [Al(μ-Me)$_2$Me$_2$] moiety can be assigned at ambient temperature.

These findings suggest two different methyl group exchange mechanisms dependent on the size of the central lanthanide cation. A sterically unsaturated rare-earth metal center allows for an associative methyl group exchange with transient η^3 coordinating [$AlMe_4$] moieties (Scheme 3, right),[33,38,39] whereas in sterically hindered complexes intramolecular methyl group exchange occurs via a dissociative mechanism with transient η^1 coordination (Scheme 3, left).[39]

Dynamic NMR spectroscopy has previously been successfully used to determine methyl group exchange rates and activation parameters of several homoleptic and heteroleptic lanthanide tetramethylaluminate complexes.[33,38,39] Therefore, the ^{1}H NMR spectra of (BDPPpyr)Sc[(μ-Me)$_2$AlMe$_2$] (**4a**) and (BDPPpyr)-Lu[(μ-Me)$_2$AlMe$_2$] (**4b**) were examined in different temperature ranges as solutions in toluene-d_8. Rate constants k of the methyl group exchange were obtained by line shape analysis of the ^{1}H methyl signals[40] and the activation parameters $\Delta G^{\ddagger}$, $\Delta H^{\ddagger}$, and $\Delta S^{\ddagger}$ were calculated from a linearized Eyring equation.[41] Accordingly, the aluminate methyl group exchange in the lutetium compound **4b** proceeds with activation parameters indicative of an associative methyl group exchange (Scheme 3, right; Table 2). The negative activation entropy $\Delta S^{\ddagger} = -56(4)$ J K^{-1} mol^{-1} implies a higher ordered transition state with an η^3-coordinated tetramethylaluminate ligand. Relatively weak aluminate bonding is proposed by the low $\Delta H^{\ddagger}$ value (34(1) kJ mol^{-1}). The activation parameters of **4b** are in very good agreement with those found for homoleptic Lu($AlMe_4$)$_3$ (**3b**).[33] The parameters obtained for the scandium complex **4a** have to be treated carefully as coalescence of the aluminate methyl signals ($T_C = 72$ °C) appeared very close to the decomposition temperature of the compound. The amount of available data points is therefore limited. Nevertheless, the activation entropy for this small metal center is clearly positive ($\Delta S^{\ddagger} = 122(1)$ J K^{-1} mol^{-1}) indicating a dissociative methyl group exchange (Scheme 3, left; Table 2) with lower ordering in the transition state (η^1-coordinated tetramethylaluminate ligand). Additionally, the high activation enthalpy $\Delta H^{\ddagger} = 109(1)$ kJ mol^{-1} is in accordance with a very strong bonding of the tetramethylaluminate ligand to the small, Lewis acidic scandium metal center. A dissociative methyl group exchange was also found for the Al_2Me_6 dimer[42] and a sterically crowded heteroleptic yttrium carboxylate complex (Table 2).[39] The comparatively increased free activation energy $\Delta G^{\ddagger}$ for the smaller metal center Sc corresponds to a slowing of the methyl group exchange, e.g., $\Delta(\Delta G^{\ddagger})$ of 23 kJ mol^{-1} at 298 K corresponds to a slowing by a factor of approximately 1×10^4, which is in good agreement with the obtained ^{1}H NMR spectra of **4a** and **4b**. Owing to enhanced steric unsaturation of the larger metal centers, associative methyl group exchange is assumed for the yttrium (**4c**) and lanthanum derivatives (**4d**).

Table 1. Selected Structural Parameters for (BDPPpyr)Lu($AlMe_4$) (4b) (Symmetry Code x, 1/2−y, z)

Bond Distances (Å)			
Lu−N1	2.336(2)	Al−C1	2.088(4)
Lu−N2	2.186(2)	Al−C2	2.103(3)
Lu−C1	2.424(3)	Al−C3	1.960(3)
Lu−C2	2.435(3)	N2−C7	1.451(3)
Lu···Al	3.001(1)	C6−C7	1.503(3)
Bond Angles (deg)			
N1−Lu−N2	70.13(4)	Lu−N2−C8	125.2(1)
N2−Lu−N2′	138.6(1)	C1−A1−C3	107.5(1)
N1−Lu−C1	150.3(1)	N1−C6−C7	115.1(2)
N1−Lu−C2	122.0(1)	C6−C7−N2	111.2(2)
Lu−C1−Al	83.0(1)		

Whereas compounds **4** precipitate cleanly from the hexane solution when reacting H_2[**1**] with Ln($AlMe_4$)$_3$ (**3**), the orange soluble fraction contains the aluminum complex (BDPPpyr)-($AlMe_2$)$_2$ (**5**) (Scheme 2) as the only byproduct besides unreacted Ln($AlMe_4$)$_3$. Fractional crystallization from hexane afforded analytically pure yellow crystals of **5** suitable for X-ray diffraction analysis. The molecular structure and relevant bond distances and angles of **5** can be found in Figure 2 and Table 3. The solid-state structure revealed a BDPPpyr ligand that is

(38) Eppinger, J. *Ph.D. Thesis*, **1999**, Technische Universität München.
(39) Fischbach, A.; Perdih, F.; Herdtweck, E.; Anwander, R. *Organometallics* **2006**, *25*, 1626.

(40) (a) Gutowsky, H. S.; Holm, C. H. *J. Chem. Phys.* **1956**, *25*, 1228. (b) Allerhand, A.; Gutowsky, H. S.; Jonas, J.; Meinzner, R. A. *J. Am. Chem. Soc.* **1966**, *88*, 3185. (c) Piette, L. H.; Anderson, W. A. *J. Chem. Phys.* **1959**, *30*, 899.
(41) $\Delta G^{\ddagger}$, $\Delta H^{\ddagger}$, and $\Delta S^{\ddagger}$ were obtained from a linearized *Eyring* plot based on $-Rln(kh/k_BT) = -\Delta S^{\ddagger} + \Delta H^{\ddagger}/T$.
(42) O'Neill, M. E.; Wade, K. In *Comprehensive Organometallic Chemistry*; Wilkinson, G., Stone, F. G. A., Abel, E. W., Eds.; Pergamon Press: New York, 1982; p. 593.

Table 2. Thermodynamic Data for the Exchange of Bridging and Terminal Methyl Groups in Tetramethylaluminate Complexes

compound	T_c [K]	$\Delta G^{\ddagger c}$ [kJ mol^{-1}]	$\Delta H^{\ddagger}$ [kJ mol^{-1}]	$\Delta S^{\ddagger}$ [J K^{-1} mol^{-1}]
(BDPPpyr)Sc[(μ-Me)$_2$AlMe$_2$] (**4a**)	345	73(1)	109(1)	122(1)
(BDPPpyr)Lu[(μ-Me)$_2$AlMe$_2$] (**4b**)	213	50(2)	34(1)	−56(4)
Lu[(μ-Me)$_2$AlMe$_2$]$_3$ (**3b**)[33]	279	51.8(3)[d]	44(1)	−30(3)
Y[(μ-Me)$_2$AlMe$_2$]$_3$ (**3c**)[33]	229	43.6(3)[d]	38(1)	−26(4)
[L^1]$_2$Y[(μ-Me)$_2$AlMe$_2$][a,39]	263	53(3)	73(4)	66(3)
[L^1]$_2$La[(μ-Me)$_2$AlMe$_2$][a,39]	213	45(2)	28(2)	−58(3)
[L^2]Y[(μ-Me)$_2$AlMe$_2$][b,38]		63.0	24.3	−130
Me$_2$Al(μ-Me)$_2$AlMe$_2$[42]		44.8	81.5	123.1

[a] L^1 = (O$_2$CAr^{iPr})$_2$(μ-AlMe$_2$). [b] L^2 = Me$_2$Si(2-MeBenzInd)$_2$. [c] Uncertainties mainly based on temperature errors. [d] T_c.

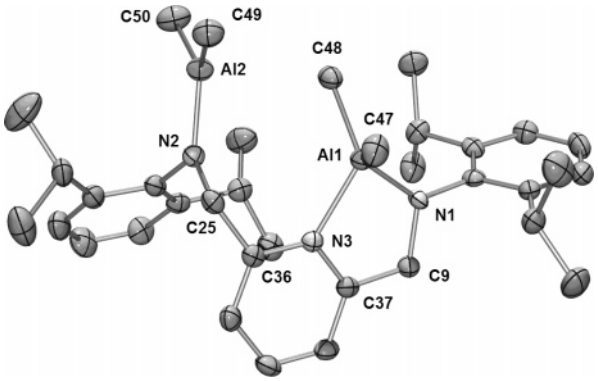

Figure 2. Molecular structure of (BDPPpyr)(AlMe$_2$)$_2$ (**5**) (atomic displacement parameters set at the 50% level). Hydrogen atoms are omitted for clarity.

Table 3. Selected Structural Parameters for (BDPPpyr)(AlMe$_2$)$_2$ (5)

	Bond Distances (Å)		
Al1−N1	1.829(3)	N3−C37	1.349(3)
Al1−N2	1.797(3)	C37−C9	1.491(5)
Al2−N3	2.005(3)	N1−C9	1.448(4)
Al1−C47	1.966(4)	N3−C36	1.363(4)
Al1−C48	1.977(4)	C36−C25	1.501(5)
Al2−C49	1.935(4)	N2−C25	1.470(4)
Al2−C50	1.930(4)		
	Bond Angles (deg)		
N1−Al1−N3	85.1(1)	C9−C37−N3	116.3(3)
N1−Al1−C47	119.5(1)	N2−Al2−C49	115.7(2)
N1−Al1−C48	114.3(1)	N2−Al2−C50	118.3(2)
N3−Al1−C47	106.3(2)	Al2−N2−C25	121.6(2)
N3−Al1−C48	119.1(1)	N2−C25−C36	113.6(3)
Al1−N1−C9	115.7(2)	C25−C36−N3	118.0(3)
N1−C9−C37	110.4(3)		

coordinated to two aluminum metal centers in an η^2 (N1 and N3) and an η^1 fashion (N2). All Al−N bond lengths and the N1−Al1−N3 bite angle are in the expected ranges.[29,43] To accommodate the second [AlMe$_2$] moiety, one CH$_2$N sidearm is tilted 74.6(4)° (torsion angle N3−C36−C25−N2) out of the plane of the ligand backbone. Broad signals for the CH$_2$N and aryl isopropyl hydrogen atoms in the ^{1}H NMR spectrum of **5** indicate high fluxionality of the ligand backbone in C$_6$D$_6$.

Formation of organoaluminum byproducts has occurred earlier during the reaction of a imino-amino-pyridine with homoleptic lanthanide tetramethylaluminates **3**.[29] So far it is not clear whether the byproduct formation is a result of an intermolecular reaction between H$_2$BDPPpyr and AlMe$_3$ released in the acid−base reaction of H$_2$[**1**] and Ln(AlMe$_4$)$_3$ or rather that of an intramolecular competition between the Lewis acidic Al^{3+} and the lanthanide metal centers for the BDPPpyr ligand. The strong Lewis acid Al^{3+} has a high affinity for nitrogen donors.[44] The evidenced Ln^{3+} size dependency of the aluminum complex formation supports the latter mechanistic scenario.[29]

C−H Bond Activation and Cyclometallation Pathways of (BDPPpyr)Ln(AlMe$_4$) Complexes. Upon stirring the reaction mixture of H$_2$[**1**] and Y(AlMe$_4$)$_3$ (**3c**) at ambient temperature, the intermediately formed (BDPPpyr)Y(AlMe$_4$) (**4c**) is gradually undergoing an intramolecular metalation process with one of the aryl-isopropyl methyl groups (Scheme 4).

The transformation is accompanied by evolution of one equivalent CH$_4$ and formation of a yellow solid material with slightly higher solubility in hexane than "reaction intermediate **4c**". Full and clean conversion to compound **6** was accomplished within 24 h and yellow single crystals suitable for X-ray diffraction analysis were grown from a hexane solution (Figure 3, Table 4). The molecular structure of **6** revealed the product of a ligand metalation via σ-bond metathesis between the C−H bond of the *i*Pr-methyl group and a bridging Y−CH$_3$ bond of the Y[(μ-CH$_3$)$_2$Al(CH$_3$)$_2$] unit, showing the overall composition (BDPPpyr-**H**)Y[(μ-Me)AlMe$_2$]$_2$. As a result, the BDPPpyr ligand coordinates in an η^4 fashion to the six-coordinate yttrium metal center. The pyridine nitrogen (N2) and one bridging carbon of the former tetramethylaluminate ligand (C32) occupy the apical positions (N2−Y−C32 = 161.94(5)°) of a strongly distorted octahedral coordination geometry. Due to the formation of one heterobridging [Y(μ-NR$_2$)(μ-Me)AlMe$_2$] moiety, the Y−N bond lengths differ considerably involving a very long Y−N1 (2.485(1) Å) and a very short Y−N3 bond of 2.191(1) Å.[28,45] Similar heterobridging units were previously described for (BDPPthf)La[(μ-Me)$_2$AlMe$_2$][(μ-Me)AlMe$_2$],[28] Nd(N*i*Pr$_2$)-[(μ-N*i*Pr$_2$)(μ-Me)AlMe$_2$][(μ-Me)$_2$AlMe$_2$],[46] {[Me$_2$Al(μ-Me)$_2$]$_2$-Nd(μ_3-NC$_6$H$_5$)(μ-Me)AlMe}$_2$,[47] and [(μ-NC$_6$H$_3$*i*Pr$_2$-2,6)Sm(μ-NHC$_6$H$_3$*i*Pr$_2$-2,6)(μ-Me)AlMe$_2$]$_2$.[48] For better understanding of the AlMe$_3$ impact on the formation of **6**, a suspension of (BDPPpyr)Y(AlMe$_4$) (**4c**) in hexane was stirred for 18 h at ambient temperature without and in the presence of 1 eq of AlMe$_3$ (Scheme 4).

In the absence of the organoaluminum compound neither metalation nor decomposition of **4c** took place, whereas complete conversion of **4c** into metalated compound **6** was found in the presence of AlMe$_3$. Therefore, it is the initial formation of the heterobridging [Y(μ-NR$_2$)(μ-Me)AlMe$_2$] unit that facilitates this metalation reaction pathway. The latter can be rationalized on the basis of kinetic (due to steric constraint)

(43) (a) Bruce, M.; Gibson, V. C.; Redshaw, C.; Solan, G. A.; White, A. J. P.; Williams, D. J. *Chem. Commun.* **1998**, 2523. (b) Scott, J.; Gambarotta, S.; Korobkov, I.; Knijnenburg, Q.; de Bruin, B.; Budzelaar, P. H. M. *J. Am. Chem. Soc.* **2005**, *127*, 17204.

(44) Duchateau, R.; van Wee, C. T.; Meetsma, A.; van Duijnen, P. T.; Teuben, J. H. *Organometallics* **1996**, *15*, 2279.

(45) Graf, D. D.; Davis, W. M.; Schrock, R. R. *Organometallics* **1998**, *17*, 5820.

(46) Evans, W. J.; Anwander, R.; Ziller, J. W. *Inorg. Chem.* **1995**, *34*, 5930.

(47) Evans, W. J.; Ansari, M. A.; Ziller, J. W.; Khan, S. I. *Inorg. Chem.* **1996**, *35*, 5435.

(48) Gordon, J. C.; Giesbrecht, G. R.; Clark, D. L.; Hay, P. J.; Keogh, D. W.; Poli, R.; Scott, B. L.; Watkin, J. G. *Organometallics* **2002**, *21*, 4726.

Scheme 4. Ligand Metalation of 4c via *σ*-bond Metathesis

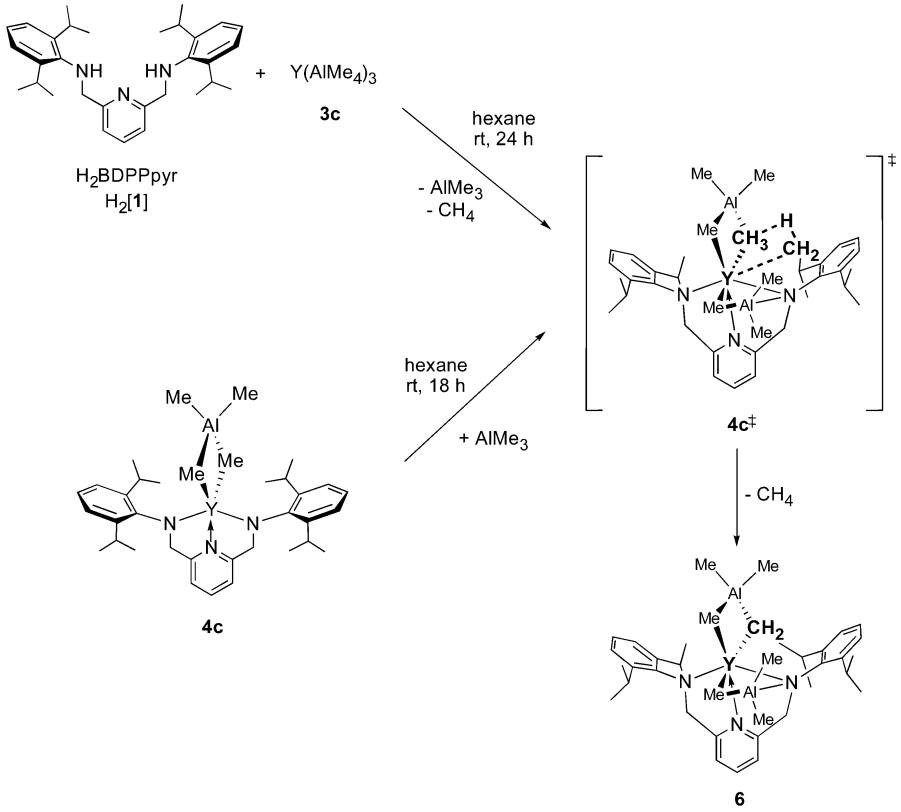

or thermodynamic control. Since the path breaking investigation by Watson et al.,[23] the capability of Ln−methyl functionalities to engage in the activation of C−H bonds has been well established. Recently, single and multiple C−H bond activation was evidenced for lanthanide mono-C_5Me_5 complexes containing tetramethylaluminate functionalities [$AlMe_4$].[49,50] In **6**, the interaction of one bridging methyl group of the tetramethylaluminate ligand with the aryl-*i*Pr group led to *σ*-bond metathetical loss of methane and concomitantly to the formation of a six-membered metalacycle as well as a mixed alkylaluminate species.

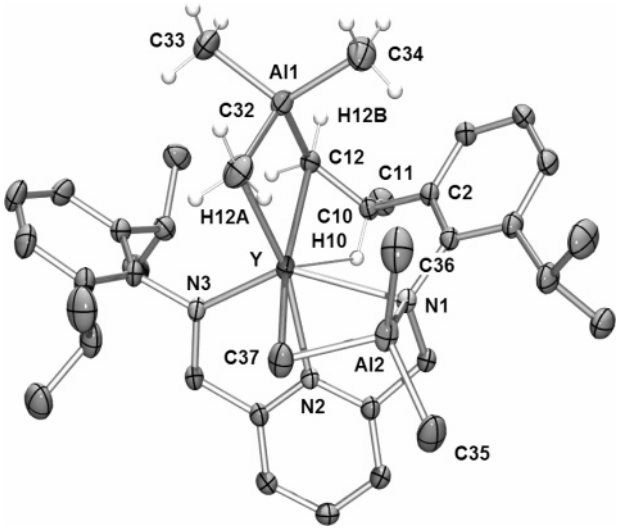

Figure 3. Molecular structure of (BDPPpyr-**H**)Y[(μ-Me)$AlMe_2$)]$_2$ (**6**) (atomic displacement parameters set at the 50% level). Hydrogen atoms (except for H10, H12A-B, H32A-C, H33A-C, and H34A-C) are omitted for clarity.

Table 4. Selected Structural Parameters for Complex (BDPPpyr-H)Y[(μ-Me)$AlMe_2$]$_2$ (6)

Bond Distances (Å)			
Y−N1	2.485(1)	Al2−C36	1.983(2)
Y−N2	2.397(1)	Al2−C37	2.063(2)
Y−N3	2.191(1)	C12−C10	1.554(2)
Y−C12	2.553(1)	C10−C2	1.523(2)
Y−C32	2.545(1)	C10−C11	1.538(2)
Y−C37	2.651(2)	C10−H10	1.00(2)
Al2−N1	1.970(1)	C12−H12A	1.00(2)
Al1−C12	2.102(2)	C12−H12B	0.93(2)
Al1−C32	2.057(2)	Y···H10	2.33(2)
Al1−C33	1.968(2)	Y···H12A	2.74(2)
Al1−C34	1.970(2)	Y···Al1	3.0769(5)
Al2−C35	1.974(4)	Y···Al2	3.1350(4)
Bond Angles (deg)			
N1−Y−N3	139.30(4)	C37−Al2−C35	103.01(7)
N1−Y−N2	69.42(3)	C37−Al2−C36	105.74(7)
N2−Y−N3	69.88(4)	Y−C12−C10	81.83(7)
N2−Y−C12	114.00(4)	C12−C10−C2	110.7(1)
N2−Y−C32	161.94(5)	C12−C10−C11	111.6(1)
N2−Y−C37	78.43(5)	Y−C12−H12A	89.9(9)
C12−Y−C37	161.88(5)	Y−C12−H12B	163(1)
Y−C12−Al1	82.14(5)	C12−C10−H10	109.3(9)
Y−C32−Al1	83.20(6)	C11−C10−H10	103.0(9)
C32−Al1−C33	104.38(8)	Y−N1−C1	110.39(7)
C32−Al1−C34	107.54(8)	Y−N3−C20	124.12(8)
Y−C37−Al2	82.36(5)		

The hydrogen atoms at the bridging methyl group (C32) and at C12 were located and refined and unequivocally proved the formation of a bridging methylene group (CH_2^-) (Figure 3). Similar reactivity has been documented for $LScR_2$ and LScR(NHR′) complexes supported by Nacnac$^-$ ligands carrying bulky 2,6-diisopropylphenyl substituents (Chart 1, **G**).[11,51]

(49) Dietrich, H. M.; Törnroos, K. W.; Anwander, R. *J. Am. Chem. Soc.* **2006**, *128*, 9298.

(50) Dietrich, H. M.; Grove, H.; Törnroos, K. W.; Anwander, R. *J. Am. Chem. Soc.* **2006**, *128*, 1458.

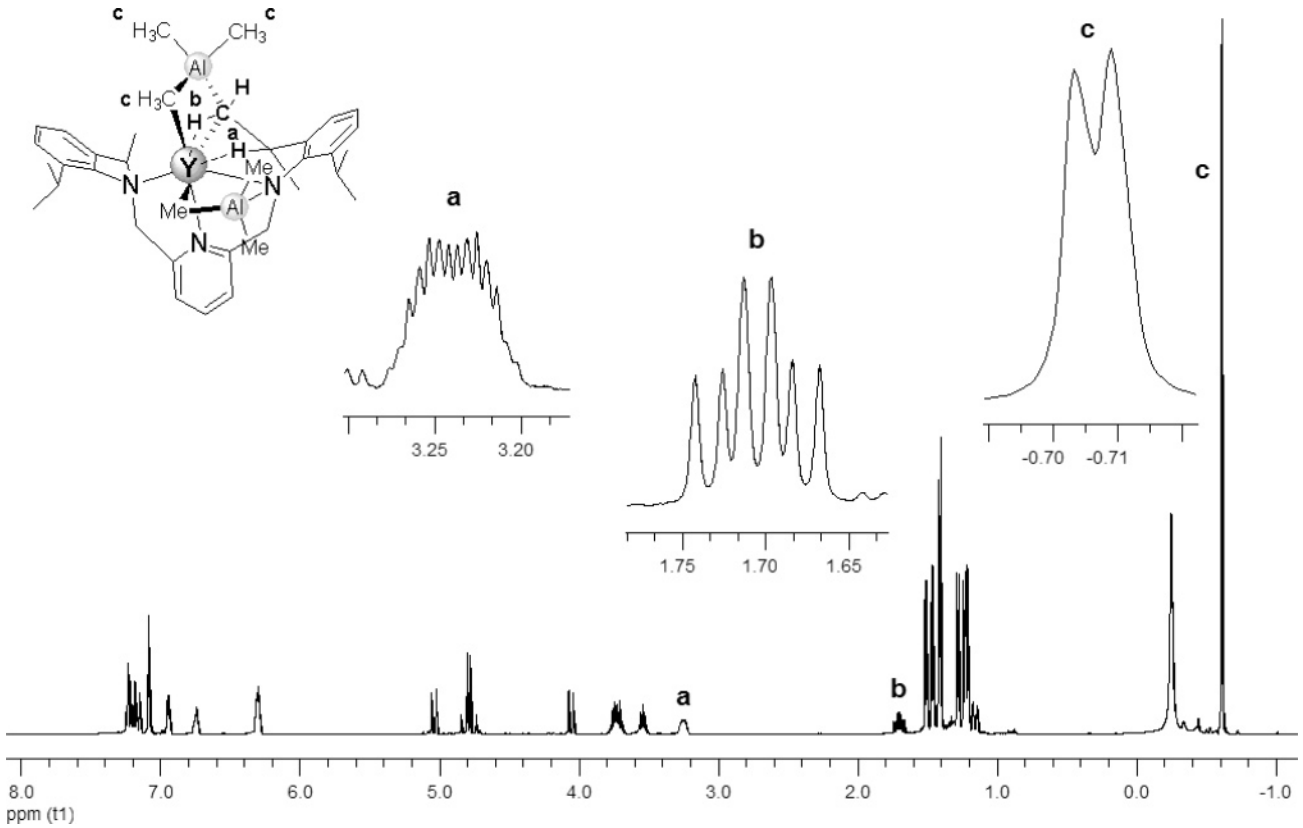

Figure 4. ^{1}H NMR spectrum (500.13 MHz) of **6** as a solution in C_6D_6 at 298 K.

The characteristic pattern of four methine multiplets and seven methyl doublets for the *i*Pr groups in the ^{1}H NMR spectrum of **6** in C_6D_6 are clearly indicative of the outcome of this reaction (Figure 4). A doublet of doublets at 1.16 ppm ($^{2}J_{HH}$ = 15.5 Hz, $^{3}J_{HH}$ = 3.5 Hz) can be assigned to one of the diastereotopic Y−CH_2 methylene protons, whereas the second methylene proton appears as a doublet of doublets of doublets (1.71 ppm), due to an additional scalar $^{1}H-^{89}Y$ coupling ($^{2}J_{HH}$ = 15.5 Hz, $^{3}J_{HH}$ = 8.0 Hz, $^{1}J_{YH}$ = 15.5 Hz) (Figure 4, **b**).[52] Scalar coupling with the ^{89}Y nucleus ($^{1}J_{YH}$ = 14.0 Hz) also leads to a doublet splitting of the multiplet at 3.24 ppm derived from the methine proton involved in the metalacycle (H10) (Figure 4, **a**). The presence of a scalar $^{1}H-^{89}Y$ coupling was further proven by ^{89}Y NMR spectroscopy (no decoupling) and 2D $^{1}H-^{89}Y$ HMQC NMR spectroscopy, showing a multiplet at 426 ppm and cross-peaks in the HMQC, respectively (Figure 5). The close Y⋯H10 contact (2.33(2) Å) in the solid-state structure of **6** is in the range of covalent Y−H bond lengths[53] and suggests an appreciable interaction in the solid state, which is retained in solution as indicated by the NMR spectroscopic investigations. A broad singlet at −0.25 ppm and a doublet at −0.71 ppm ($^{2}J_{YH}$ = 1.2 Hz) can be assigned to the two [$AlMe_3$] moieties (Figure 4, **c**). A VT NMR study of compound **6** was hampered by its rapid crystallization in toluene-d_8 below −30 °C.

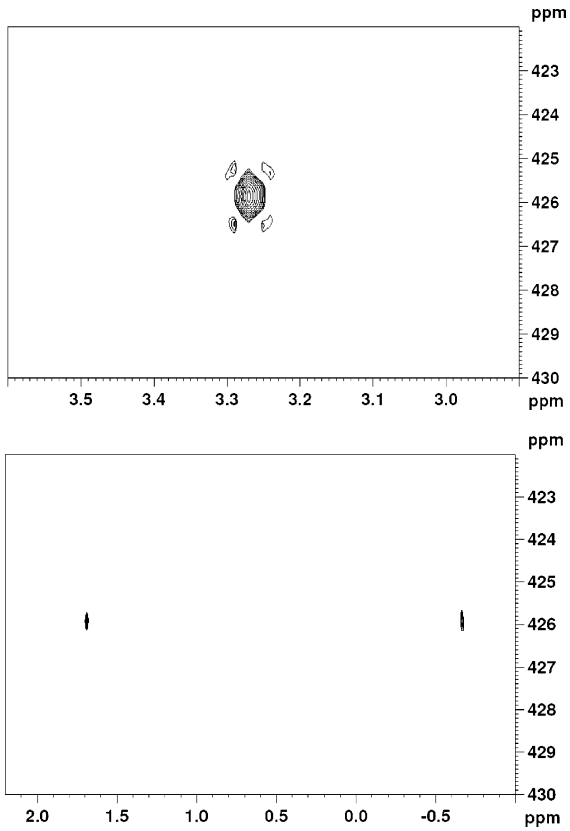

Figure 5. Two-dimensional $^{1}H-^{89}Y$ HMQC NMR spectra of **6** dissolved in toluene-d_8 at 298 K. Experiment optimized for $^{1}J_{YH}$ = 14.0 Hz (top). Experiment optimized for $^{2}J_{YH}$ = 1.5 Hz (bottom).

In contrast, the formation of analogous metalation products of the smaller and larger lanthanide metal centers scandium, lutetium and lanthanum, respectively, was not observed. Even

(51) Hayes, P. G.; Piers, W. E.; Lee, L. W. M.; Knight, L. K.; Parvez, M.; Elsegood, M. R. J.; Clegg, W. *Organometallics* **2001**, *20*, 2533.

(52) $^{1}J_{YH}$ coupling constants are in the range of 15−30 Hz: Rheder, D. In *Transition Metal Nuclear Magnetic Resonance*; Pregostin, P. S., Ed.; Elsevier: Amsterdam, 1991; pp 4−51.

(53) Examples of Y−H bond lengths from X-Ray diffraction data include the following: (a) 2.19/2.17 Å in $[(C_5H_4Me)_2Y(\mu\text{-}H)(THF)]_2$: Evans, W. J.; Meadows, J. H.; Wayda, A. L.; Hunter, W. E.; Atwood, J. L. *J. Am. Chem. Soc.* **1982**, *106*, 2008. (b) 2.35 Å in $[(C_5H_5)_2Y(\mu\text{-}Cl)]_2(\mu\text{-}H)AlH_2(OEt_2)$: Lobovskii, B.; Soloveichik, G. L.; Erofeev, A. B.; Bulichev, B. M.; Bel'skii, V. K. *J. Organomet. Chem.* **1982**, *299*, 67. (c) 2.09/2.13 Å in $[Me_2Si(2\text{-}MeC_9H_5)_2Y(THF)(\mu\text{-}H)]_2$: Klimpel, M. G.; Sirsch, P.; Scherer, W.; Anwander, R. *Angew. Chem., Int. Ed.* **2003**, *42*, 574.

Scheme 5. Donor-Induced Cleavage of the Tetramethylaluminate Ligand of 4b Followed by Ligand Metalation via σ-Bond Metathesis

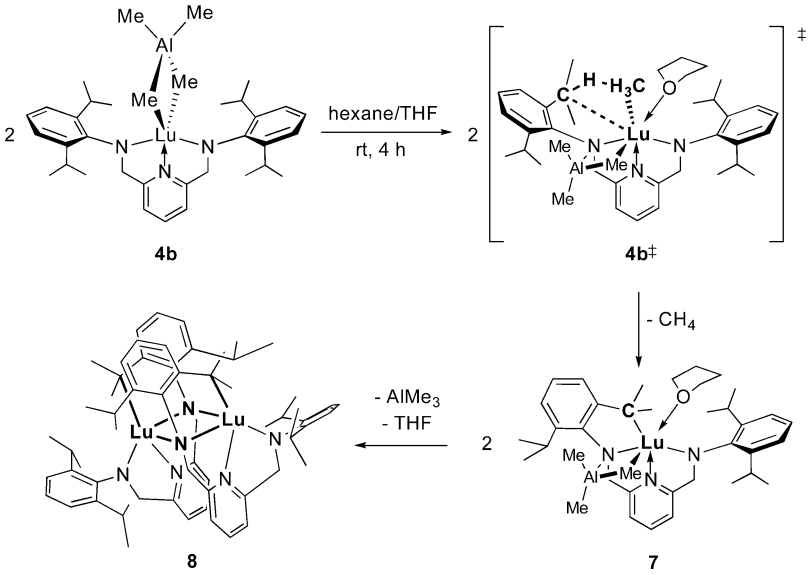

after stirring hexane suspensions of **4b** and **4d** in the presence of $AlMe_3$ for several days, the starting compounds could be recovered in almost quantitative yields. Clearly, the observed reactivity emphasizes the impact of the lanthanide cation size on the complex stability of (BDPPpyr)Ln($AlMe_4$) (**4**).

The donor-induced cleavage of tetramethylaluminate complexes (donor = THF, diethyl ether, pyridine) offers a convenient synthesis approach toward highly reactive [Ln−Me] moieties as reported for homoleptic tris(tetramethylaluminate) complexes[54] and for heteroleptic lanthanidocene and halflanthanidocene complexes, [Cp′$_2$Ln(AlR_4)] and [Cp′Ln(AlR_4)$_2$] (Cp′ = substituted cyclopentadienyl; R = Me, Et).[55,56] When treating a stirred suspension of tetramethylaluminate complex (BDPPpyr)Lu($AlMe_4$) (**4b**) in hexane with an excess of THF (Scheme 5), instant dissolution of the off-white solid occurred accompanied by a red coloration of the solution. Depending on the reaction and crystallization time, two different batches of yellow single crystals could be harvested from hexane solutions and identified by X-ray diffraction as the cyclometallation products **7** and **8** (Figures 6 and 7). Selected bond distances and angles are listed in Tables 5 and 6.

The formation of final product [Lu(BDPPpyr-**H**)]$_2$ (**8**) originates from sequential processes involving an initial donor-induced cleavage of the tetramethylaluminate ligand in complex **4b** to produce a transition structure **4b**‡ containing a highly reactive terminal methyl group and a heterobridging [Lu(μ-NR_2)(μ-Me)$AlMe_2$] unit, which seems to be vital to facilitate a metalation reaction pathway. Subsequent σ-bond metathesis between the Lu−CH_3 bond and the C−H bond of one *i*Pr-methine group of the BDPPpyr ligand results in loss of methane and consequent formation of a five-membered metalacycle of the composition (BDPPpyr-**H**)Lu[(μ-Me)$AlMe_2$]-(THF) (**7**). An X-ray structural analysis of "reaction intermediate" **7** was carried out, revealing the additional coordination of the cleaving agent THF to the lutetium metal center (Figure 6). An increased coordination number of the lutetium metal center in **7** compared to precursor complex **4b** (CN 6 versus 5) combined with ring strain caused by the fused metalacycles leads to considerably elongated Lu−C and Lu−N(amido) bond lengths (e.g., Lu−C22, 2.589(9), Lu−N3 2.432(5) Å).[57]

Finally, loss of the heterobridging $AlMe_3$ unit and displacement of coordinated THF by bridging amido moieties lead to a dimerization to form complex **8**. The two Lu metal centers seem to be perfectly embedded into two new tetradentate [**N**N**N**C]$^{3-}$ ligands which coordinate in a $\mu,\eta^4{:}\eta^1$ fashion. The coordination geometry of the five-coordinate lutetium centers is best described as strongly distorted trigonal bipyramidal with the two amido nitrogen atoms (N1 and N3) occupying the apical positions (N1−Lu1−N3 = 138.82(6)°) and the pyridine N2 atom, the methine carbon (C29), and the bridging amido nitrogen of the second ligand (N3′) spanning the equatorial plane. Although the proneness of Ln−CH_3 bonds to undergo σ-bond metathetical loss of methane is well documented,[4,23,49−51,58,59] C−H abstraction at a methine group (*tert*. carbon) is statistically and kinetically disfavored and therefore exceedingly rare.[58] To our knowledge, complexes **7** and **8** are the first examples of a structurally authenticated activation of a methine group within organolanthanide chemistry (e.g., derived from Pt, Fe, and Ti, see Chart 1, **D**, **E**, and **F**).[9,10,60]

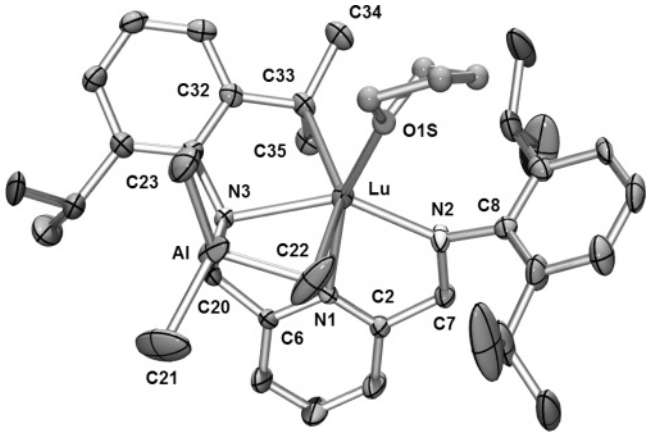

Figure 6. Molecular structure of reaction intermediate (BDPPpyr-**H**)Lu[(μ-Me)$AlMe_2$](THF) (**7**) (atomic displacement parameters set at the 50% level). Hydrogen atoms are omitted for clarity.

(54) Dietrich, H. M.; Raudaschl-Sieber, G.; Anwander, R. *Angew. Chem., Int. Ed.* **2005**, *44*, 5303.

(55) Holton, J.; Lappert, M. F.; Ballard, D. G. H.; Pearce, R.; Atwood, J. L.; Hunter, W. E. *J. Chem. Soc., Dalton Trans* **1979**, 54.

(56) Klimpel, M. G.; Eppinger, J.; Sirsch, P.; Scherer, W.; Anwander, R. *Organometallics* **2002**, *21*, 4021.

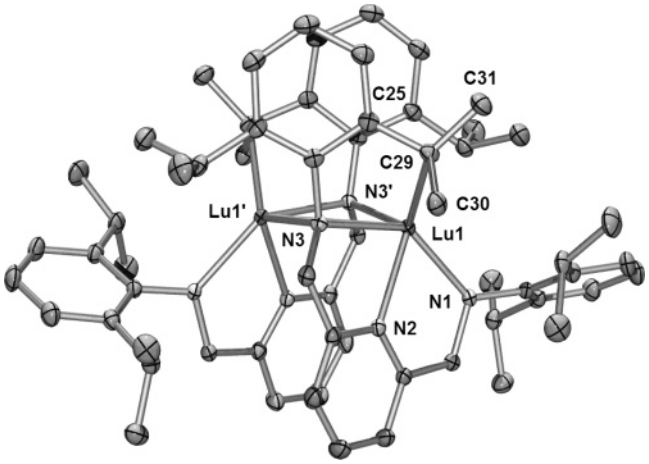

Figure 7. Molecular structure of dimeric [Lu(BDPPpyr-**H**)]$_2$ (**8**) (atomic displacement parameters set at the 50% level). Hydrogen atoms are omitted for clarity.

Table 5. Selected Structural Parameters for Complex (BDPPpyr-H)Lu[(μ-Me)AlMe$_2$](THF) (7)

Bond Distances (Å)			
Lu−N1	2.337(4)	Al−C23	1.971(7)
Lu−N2	2.209(5)	C33−C34	1.538(8)
Lu−N3	2.432(5)	C33−C35	1.550(8)
Lu−C33	2.373(6)	N2−C8	1.461(13)
Lu−C22	2.589(9)	N2−C7	1.441(7)
Lu−O1S	2.284(7)	C2−C7	1.500(8)
Lu···Al	3.102(2)	N1−C2	1.336(7)
Lu···H22A	2.39(8)	N1−C6	1.355(7)
Al−N3	1.955(5)	C6−C20	1.494(8)
Al−C21	1.974(9)	N3−C20	1.489(8)
Al−C22	2.047(9)		
Bond Angles (deg)			
N2−Lu−N3	141.28(16)	Lu−N3−C24	109.6(3)
N1−Lu−N2	70.84(16)	Lu−C33−C32	106.6(4)
N1−Lu−N3	70.44(15)	Lu−N2−C8	127.5(12)
N1−Lu−O1S	160.5(2)	N3−Al−C22	103.6(3)
N1−Lu−C33	103.00(18)	C22−Al−Lu	56.0(2)

Table 6. Selected Structural Parameters for Complex [Lu(BDPPpyr-H)]$_2$ (8) (Symmetry Code $-x, y, 3/2-z$)

Bond Distances (Å)			
Lu1−N1	2.249(2)	Lu1−C29	2.399(2)
Lu1−N2	2.350(2)	C29−C25	1.498(3)
Lu1−N3	2.338(2)	C29−C30	1.550(3)
Lu1−N3′	2.318(2)	C29−C31	1.530(3)
Bond Angles (deg)			
N1−Lu1−N3	138.82(6)	N3−Lu1−N3′	82.99(6)
N1−Lu1−N2	70.77(6)	Lu1′−N3−Lu1	96.01(6)
N2−Lu1−N3	68.19(6)	N2−Lu1−C29	114.78(6)
N1−Lu1−N3′	105.67(6)	Lu1−C29−C30	95.9(1)
N2−Lu1−N3′	106.36(6)	Lu1−C29−C31	130.8(2)

The ^{1}H NMR spectroscopic investigation of **8** hallmark the metalated compound as the spectrum revealed only three septets at 3.76, 3.68, and 3.11 ppm for the remaining *i*Pr-methine protons and further two singlets at 1.36 and 1.24 ppm that can be assigned to the noncoupling LuC(CH_3) protons. A signal at 95.1 ppm in the ^{13}C CAPT NMR spectrum of **8** further underlines the presence of a quaternary carbon atom.

Attempted donor-induced cleavage of the tetramethylaluminate ligand in the Sc (**4a**), Y (**4c**), and La (**4d**) complexes even with weaker (diethyl ether) or stronger (pyridine) donors than THF did not result in well-defined, characterizable products but in extensive ligand degradation. Again, these findings emphasize a sensitive and distinct cation size/reactivity correlation as well as the extremely high reactivity of terminal Ln−methyl groups.

Conclusions

Complexes (BDPPpyr)Ln[(μ-Me)$_2$AlMe$_2$] were synthesized following an amide elimination protocol (Ln = Sc, Lu) or via the "aluminate route" using homoleptic Ln(AlMe$_4$)$_3$ as lanthanide alkyl precursors (Ln = Lu, Y, La). Application of the two synthesis approaches gave access to the entire size range of rare-earth metal centers (Sc−La), thus allowing for comprehensive insight into the intrinsic properties, metal-size dependent dynamic behavior, and reactivity of the resulting tetramethylaluminate complexes. Dynamic ^{1}H NMR spectroscopy and lineshape analysis evidenced a dissociative exchange of bridging and terminal methyl groups of the tetramethylaluminate ligand in the sterically crowded (BDPPpyr)Sc(AlMe$_4$) (lower ordered transient state, η^1), whereas negative values of $\Delta S^{\ddagger}$ were calculated for the lutetium derivative, substantiating an associative exchange with a η^3 transient state. Because of the intrinsic interrelation of group 4 and group 3/lanthanide metal chemistry, complexes (BDPPpyr)Ln(AlMe$_4$) might be considered as model systems to reveal mechanistic details of post-metallocene based polymerization processes. In the presence of cocatalysts like MAO or organoaluminum reagents, tetraalkylaluminate complexes are proposed as polymerization retarding species ("dormant species"). They are further discussed as important intermediates in chain transfer and termination processes as β-H elimination, β-alkyl elimination via C−H activation and σ-bond metathesis processes. Ancillary ligand degradation via intramolecular σ-bond metathetical C−H activation as herein structurally and spectroscopically evidenced for (BDPPpyr)Y(AlMe$_4$), hence, exhibits a possible catalyst deactivation scenario in the respective group 4 catalyst mixtures. Given that this gradual ligand degradation is initiated by excess of organoaluminum cocatalyst and that it can be very slow, polymerization set-ups involving (prolonged) catalyst aging procedures should be viewed very critically ("single-site" catalysts). The formation of highly reactive [Ln−Me] moieties in the presence of small amounts of donor solvent and their unpredictable nature is impressively substantiated by an unprecedented C−H activation of a methine group. Due to the high affinity of Lewis acidic Al^{3+} to nitrogen donors, the formation of aluminum byproducts like the characterized (BDPPpyr)(AlMe$_2$)$_2$ should be anticipated for post-metallocene systems, particularly for those derived form *N*-donor ancillary ligands. Their role as possible chain transfer reagents has to be discussed. Clearly, the present (rare-earth) metal-size dependent activation/degradation processes once more emphasize the sensitivity of catalyst/cocatalyst systems to small stereoelectronic modifications and the complexity of Ziegler catalyst mixtures.

Experimental Section

All operations were performed with rigorous exclusion of air and water, using standard Schlenk, high-vacuum, and glovebox

(57) Representative Lu−C bond lengths from X-ray diffraction data include the following: (a) av. 2.361 Å in 5-coordinate Lu(CH$_2$SiMe$_3$)$_2$(THF)$_2$: ref. 34d. (b) 2.477−2.573 Å in 6-coordinate LuMe$_3$(LiMe)$_3$(DME)$_3$: Schumann, H.; Lauke, H.; Hahn, E.; Pickardt, J. *J. Organomet. Chem.* **1984**, *263*, 29.

(58) (a) Crowther, D. J.; Baenziger, N. C.; Jordan, R. F. *J. Am. Chem. Soc.* **1991**, *113*, 1455. (b) Den Haan, K. H.; Wielstra, Y.; Teuben, J. H. *Organometallics* **1987**, *6*, 2053.

(59) (a) Labinger, J. A.; Bercaw, J. E. *Nature* **2002**, *417*, 507. (b) Stahl, S. S.; Labinger, J. A.; Bercaw, J. E. *Angew. Chem., Int. Ed.* **1998**, *37*, 2180.

(60) C−H abstraction at both the methine and methyl group occurred for (a) (Nacnac)Pt(IV)Me$_3$: Fekl, U.; Goldberg, K. I. *J. Am. Chem. Soc.* **2002**, *124*, 6804. (b) (AnIm)Pt(IV)Me$_3$: ref. 7.

techniques (MBraun MBLab; <1 ppm O_2, <1 ppm H_2O). Hexane, THF, and toluene were purified by using Grubbs columns (MBraun SPS, solvent purification system) and stored in a glovebox. C_6D_6 and toluene-d_8 were obtained from Aldrich, degassed, dried over Na for 24 h, and filtered. $AlMe_3$ was purchased from Aldrich and used as received. (BDPPpyr)Ln(NEt_2)(THF) (Ln = Sc, Lu) (**2**),[18] 2,6-bis(((2,6-diisopropylphenyl)amino)methyl)pyridine (H_2BDPPpyr, H_2[**1**]),[15] and Ln($AlMe_4$)$_3$ (Ln = Lu, Y, La) (**3**)[33,54,61] were synthesized according to the literature methods. ^{1}H and ^{13}C NMR spectra were recorded at 25 °C on a Bruker-BIOSPIN-AV500 (5 mm BBO, ^{1}H: 500.13 Hz; ^{13}C: 125.77 MHz) and a Bruker-BIOSPIN-AV600 (5 mm cryo probe, ^{1}H: 600.13 MHz; ^{13}C: 150.91 MHz). ^{1}H and ^{13}C shifts are referenced to internal solvent resonances and reported in parts per million relative to TMS. ^{89}Y NMR experiments were performed on the AV500 (24.51 MHz, ^{1}H inverse gated decoupling). The ^{1}H-detected ^{1}H−^{89}Y HMQC spectra[62] were acquired in the pure-absorption mode. Because ^{89}Y is present at 100% natural abundance, no gradients were required for coherence selection. Thirty-two t_1 increments were collected, 4 transients were averaged for each increment, and the recycling delay was 2 s. The experiment was optimized for $^2J_{HY}$ = 1.5 Hz and $^1J_{HY}$ = 14 Hz. Broadband ^{89}Y decoupling (composite pulse decoupling) was used during the acquisition and the Ξ-scale was used for referencing the ^{89}Y chemical shift.[63] IR spectra were recorded on a NICOLET Impact 410 FTIR spectrometer as Nujol mulls sandwiched between CsI plates. Elemental analyses were performed on an Elementar Vario EL III.

General Procedure for the Synthesis of (BDPPpyr)Ln($AlMe_4$) (4a,b) from (BDPPpyr)Ln(NEt_2)(THF) (2a,b). In a glovebox, 3 eq $AlMe_3$ were added dropwise to a stirred solution of **2** in 5 mL of hexane at ambient temperature. The reaction mixture was stirred another 3 h at ambient temperature while the formation of a white precipitate was observed. The product was separated by centrifugation and washed three times with 2 mL of hexane to yield **4** as powdery off-white solids in almost quantitative yields. Crystallization from a hexane/toluene solution at −35 °C gave colorless crystals of **4** in moderate yields suitable for X-ray diffraction analysis.

(BDPPpyr)Sc($AlMe_4$) (4a). Following the procedure described above, $AlMe_3$ (32 mg, 0.45 mmol) and (BDPPpyr)Sc(NEt_2)(THF) (**2a**) (97 mg, 0.15 mmol) yielded **4a** (88 mg, 0.15 mmol, 99%) as colorless crystals. ^{1}H NMR (500 MHz, C_6D_6, 25 °C): δ = 7.2−7.1 (m, 6 H, ar), 6.97 (dd, $^3J \cong 8$ Hz, 1 H, pyr), 6.51 (d, $^3J \cong 8$ Hz, 2 H, pyr), 4.72 (s, 4 H, N−CH_2), 3.42 (sp, $^3J \cong 7$ Hz, 4 H, ar-CH), 1.34 (d, $^3J \cong 7$ Hz, 12 H, ar-CH_3), 1.17 (d, $^3J \cong 7$ Hz, 12 H, ar-CH_3), 0.35 (s, 6 H, Al(μ-CH_3)$_2$(CH_3)$_2$), −1.11 (s, 6 H, Al(μ-CH_3)$_2$(CH_3)$_2$) ppm. ^{13}C {^{1}H} NMR (126 MHz, C_6D_6, 25 °C): δ = 164.7, 149.0, 145.3, 137.6, 125.4, 124.4, 117.4 (C_{ar}), 65.6 (N−CH_2), 28.6, 28.2, 23.3 (CH_3, ar-CH), 16.5 (Al(μ-CH_3)$_2$(CH_3)$_2$), −9.1 (Al(μ-CH_3)$_2$(CH_3)$_2$) ppm. Anal. calcd for $C_{35}H_{53}N_3AlSc$ (587.763): C, 71.52; H, 9.09; N, 7.15. Found: C, 72.41; H, 9.20; N, 7.6.

(BDPPpyr)Lu($AlMe_4$) (4b). Following the procedure described above, $AlMe_3$ (115 mg, 1.59 mmol) and (BDPPpyr)Lu(NEt_2)(THF) (**2b**) (411 mg, 0.53 mmol) yielded **4b** (379 mg, 0.53 mmol, 99%) as colorless crystals. IR (Nujol, cm^{-1}): 1615 m, 1582 m, 1461 vs Nujol, 1379 vs Nujol, 1306 m, 1245 m, 1185 s, 1162 s, 1129 m, 1102 m, 1069 m, 1041 m, 1024 m, 953 m, 931 w, 897 w, 870 w, 837 w, 809 w, 787 m, 771 s, 726 s, 704 s, 632 m, 577 w, 550 w, 522 w. ^{1}H NMR (500 MHz, C_6D_6, 25 °C): δ = 7.26−6.95 (m, 6 H, ar), 6.92 (dd, $^3J \cong 8$ Hz, 1 H, pyr), 6.51 (d, $^3J \cong 8.0$ Hz, 2 H, pyr), 4.92 (s, 4 H, N−CH_2), 3.53 (sp, $^3J \cong 7.0$ Hz, 4 H, ar-CH), 1.33 (d, $^3J \cong 7.0$ Hz, 12 H, ar-CH_3), 1.21 (d, $^3J \cong 7.0$ Hz, 12 H, ar-CH_3), −0.33 (s br, 12 H, Al(CH_3)$_4$) ppm. ^{13}C {^{1}H} NMR (126 MHz, C_6D_6, 25 °C): δ = 165.8, 148.7, 146.2, 137.3, 125.0, 124.1, 117.6 (C_{ar}), 66.1 (N−CH_2), 28.5, 28.2, 23.4 (CH_3, ar-CH), 2.6 (Al(CH_3)$_4$) ppm. Anal. calcd for $C_{35}H_{53}N_3AlLu$ (717.778): C, 58.57; H, 7.44; N, 5.85. Found: C, 58.43; H, 7.20; N, 5.91.

General Procedure for the Synthesis of (BDPPpyr)Ln($AlMe_4$) (4b,c,d) from Ln($AlMe_4$)$_3$ (3). In a glovebox, Ln($AlMe_4$)$_3$ (**3**) was dissolved in 3 mL of hexane and added to a stirred solution of 1 equiv H_2BDPPpyr (H_2[**1**]) in 5 mL of hexane. Instant gas formation was observed. The reaction mixture was stirred another 4 h at ambient temperature while the formation of an off-white precipitate was observed. The product was separated by centrifugation and washed three times with 5 mL of hexane to yield **4** as powdery off-white solids in good yields. The remaining solids were crystallized from a hexane/toluene solution at −35 °C to give colorless crystals of **4** in moderate yields suitable for X-ray diffraction analyses.

(BDPPpyr)Lu($AlMe_4$) (4b). Following the procedure described above, Lu($AlMe_4$)$_3$ (**3b**) (221 mg, 0.51 mmol) and H_2BDPPpyr (H_2-[**1**]) (231 mg, 0.51 mmol) yielded **4b** (264 mg, 0.37 mmol, 73%) as colorless crystals.

(BDPPpyr)Y($AlMe_4$) (4c). Following the procedure described above, Y($AlMe_4$)$_3$ (**3c**) (227 mg, 0.65 mmol) and H_2BDPPpyr (H_2-[**1**]) (299 mg, 0.65 mmol) yielded **4c** (310 mg, 0.49 mmol, 75%) as colorless crystals. IR (Nujol, cm^{-1}): 1610 m, 1576 m, 1461 vs Nujol, 1379 vs Nujol, 1306 m, 1262 m, 1256 m, 1207 m, 1185 s, 1161 s, 1129 m, 1102 m, 1063 m, 1041 m, 1022 m, 958 m, 936 w, 897 w, 859 w, 815 w, 776 s, 726 s, 594 w. ^{1}H NMR (500 MHz, C_6D_6, 25 °C): δ = 7.18−7.15 (m, 6 H, ar), 6.97 (dd, $^3J \cong 8$ Hz, 1 H, pyr), 6.54 (d, $^3J \cong 8.0$ Hz, 2 H, pyr), 4.80 (s, 4 H, N−CH_2), 3.43 (sp, $^3J \cong 7.0$ Hz, 4 H, ar-CH), 1.33 (d, $^3J \cong 7.0$ Hz, 12 H, ar-CH_3), 1.21 (d, $^3J \cong 7.0$ Hz, 12 H, ar-CH_3), −0.53 (d, $^2J_{YH} \cong 3$ Hz, 12 H, Al(CH_3)$_4$) ppm. ^{13}C {^{1}H} NMR (126 MHz, C_6D_6, 25 °C): δ = 165.4, 147.6, 146.0, 137.4, 125.1, 124.3, 117.6 (C_{ar}), 65.9 (N−CH_2), 28.6, 28.3, 23.4 (CH_3, ar-CH), 1.8 (Al(CH_3)$_4$) ppm. Anal. calcd for $C_{35}H_{53}N_3AlY$ (631.713): C, 66.55; H, 8.46; N, 6.65. Found: C, 66.81; H, 8.85; N, 6.40.

(BDPPpyr)La($AlMe_4$) (4d). Following the procedure described above, La($AlMe_4$)$_3$ (**3d**) (105 mg, 0.26 mmol) and H_2BDPPpyr (H_2-[**1**]) (120 mg, 0.26 mmol) yielded **4d** (310 mg, 0.21 mmol, 81%) as colorless crystals. IR (Nujol, cm^{-1}): 1604 m, 1571 m, 1466 vs Nujol, 1378 vs Nujol, 1306 m, 1240 m, 1207 m, 1201 s, 1162 s, 1113 m, 1058 s, 1019 m, 964 w, 936 w, 897 w, 853 w, 804 w, 771 s, 732 s, 621 m, 550 w, 539 w. ^{1}H NMR (600 MHz, C_6D_6, 25 °C): δ = 7.17−7.01 (m, 6 H, ar), 7.00 (dd, $^3J \cong 7.8$ Hz, 1 H, pyr), 6.60 (d, $^3J \cong 7.8$ Hz, 2 H, pyr), 4.99 (s, 4 H, N−CH_2), 3.20 (sp, $^3J \cong 7.2$ Hz, 4 H, ar-CH), 1.34 (d, $^3J \cong 7.2$ Hz, 12 H, ar-CH_3), 1.19 (d, $^3J \cong 7.2$ Hz, 12 H, ar-CH_3), −0.46 (s, 12 H, Al(CH_3)$_4$) ppm. ^{13}C {^{1}H} NMR (151 MHz, C_6D_6, 25 °C): δ = 165.6, 147.3, 146.3, 137.5, 125.1, 124.7, 117.4 (C_{ar}), 67.4 (N−CH_2), 29.0, 27.7, 24.1 (CH_3, ar-CH), 2.7 (Al(CH_3)$_4$) ppm. Anal. calcd for $C_{35}H_{53}N_3AlLa$ (681.718): C, 61.67; H, 7.84; N, 6.16. Found: C, 61.46; H, 7.59; N, 5.85.

Synthesis of (BDPPpyr)($AlMe_2$)$_2$ (5). Following the procedure described for the synthesis of compounds **4** from Ln($AlMe_4$)$_3$ (**3**), the orange supernatant and the hexane washing solutions were combined and dried under vacuum yielding a yellow powdery solid which was redissolved in hexane. Crystallization from hexane at −30 °C gave yellow crystals of **5** in yields depending on the lanthanide metal size (Ln = Lu 27%, Y 25%, La 19% calculated on Ln($AlMe_4$)$_3$). IR (Nujol, cm^{-1}): 1615 m, 1576 m, 1455 vs Nujol, 1378 vs Nujol, 1312 m, 1256 m, 1185 m, 1162 m, 1118 m, 1091 m, 1063 m, 1035 m, 1024 w, 964 w, 936 w, 914 w, 853 w, 809 w, 771 s, 732 s, 649 m, 572 w. ^{1}H NMR (600 MHz, C_6D_6, 25 °C): δ = 7.28−7.02 (m, 6 H, ar), 6.52 (dd, $^3J \cong 7.8$ Hz, 1 H, pyr), 6.21 (d, $^3J \cong 7.8$ Hz, 2 H, pyr), 4.51 (s, 2 H, N−CH_2), 4.43 (s, 2 H,

(61) Fischbach, A.; Klimpel, M. G.; Widenmeyer, M.; Herdtweck, E.; Scherer, W.; Anwander, R. *Angew. Chem., Int. Ed.* **2004**, *43*, 2234.

(62) (a) Müller, L. *J. Am. Chem. Soc.* **1979**, *101*, 4481. (b) Bax, A.; Griffey, R. H.; Hawkins, B. L. *J. Magn. Reson.* **1983**, *55*, 301.

(63) Harris, R. K.; Becker, E. D.; Cabral de Menezes, S. M.; Goodfellow, R.; Granger, P. *Pure Appl. Chem.* **2001**, *73*, 1795.

Table 7. Crystallographic Data for Compounds 4b, 5, 6, 7, and 8

compound	4b	5	6	7	8
formula	$C_{35}H_{53}N_3AlLu{\cdot}C_6H_{14}$	$C_{35}H_{53}N_3Al_2$	$C_{37}H_{58}N_3Al_2Y$	$C_{38}H_{57}N_3OAlLu$	$C_{62}H_{80}N_6Lu_2$
fw	803.93	569.76	687.73	773.82	1259.26
color/habit	none/prism	none/lath	none/rhomb	yellow/prism	yellow/prism
crystal dim. (mm^3)	0.25 × 0.25 × 0.15	0.25 × .075 × 0.04	0.35 × 0.30 × 0.17	0.106 × 0.09 × 0.026	0.25 × 0.06 × 0.05
crystal system	orthorhombic	monoclinic	monoclinic	monoclinic	monoclinic
space group	*Pnma*	$P2_1/c$	$P2_1/n$	$P2_1/c$	$C2/c$
a, Å	13.5889(4)	21.1535(13)	11.2525(5)	10.0267(4)	19.0980(8)
b, Å	16.4035(5)	9.1668(6)	23.1905(9)	12.5492(4)	17.7147(7)
c, Å	18.5564(6)	18.287(1)	15.2776(6)	28.8528(1)	17.2840(7)
α, deg	90	90	90	90	90
β, deg	90	101.919(1)	105.627(1)	94.243(1)	112.208(1)
γ, deg	90	90	90	90	90
V, $Å^3$	4136.3(2)	3469.6(4)	3839.3(3)	3620.5(2)	5413.7(4)
Z	4	4	4	4	4
T, K	123	123	123	103	123
D_{calc},mg m^{-3}	1.291	1.091	1.190	1.420	1.545
μ, mm^{-1}	2.437	0.110	1.592	2.783	3.671
F(000)	1672	1240	1464	1592	2544
θ range, deg	2.20−30.26	2.28−25.08	2.24−30.09	2.15−25.06	2.30−30.06
index ranges (*h, k, l*)	−19/19,−23/23, −24/26	−25/25,−10/10, −21/21	−15/15,−32/32, −21/21	−11/11,−14/14, −34/34	−26/26,−24/24, −24/24
no. of rflns collected	60008	39476	64958	41264	45359
no. of indep rflns/R_{int}	6373/0.0321	6145/0.1960	11275/0.0373	6409/0.0501	7940/0.0354
no. of obsd rflns ($I > 2\sigma(I)$)	5486	3052	9194	5320	6759
data/restraints/params	6373/14/249	6145/0/373	11275/9/426	6409/226/496	7940/0/323
*R*1/*wR*2 ($I > 2\sigma(I)$)[a]	0.0218/0.0516	0.0544/0.0977	0.0272/0.0651	0.0399/0.0950	0.0190/0.0419
*R*1/*wR*2 (all data)[a]	0.0303/0.0561	0.1560/0.1332	0.0410/0.0708	0.0522/0.1018	0.0283/0.0453
GOF (on F^2)[a]	1.070	0.987	1.028	1.042	1.023
largest diff peak and hole (e $Å^{-3}$)	1.79/−0.92	0.28/−0.28	0.38/−0.51	3.18/−0.47	0.93/−0.69

[a] $R1 = \sum(||F_0| - |F_c||)/\sum|F_0|$; $wR2 = \{\sum[w(F_0^2 - F_c^2)^2]/\sum[w(F_0^2)^2]\}^{1/2}$; GOF $= \{\sum[w(F_0^2 - F_c^2)^2]/(n - p)\}^{1/2}$.

N−CH_2), 3.87 (m, 2 H, ar-CH), 3.33 (m, 2 H, ar-CH), 1.40 (s br, 6 H, ar-CH_3), 1.37 (s br, 6 H, ar-CH_3), 1.16 (s br, 6 H, ar-CH_3), 0.88 (s br, 6 H, ar-CH_3), −0.06 (s br, 6 H, Al(CH_3)$_2$), −0.38 (s br, 6 H, Al(CH_3)$_2$) ppm. ^{13}C {^1H} NMR (151 MHz, C_6D_6, 25 °C): *δ* = 157.9, 148.7, 147.7, 145.7, 139.0, 126.3, 126.2, 124.1, 120.8 (C_{ar}), 60.2, 57.7 (N−CH_2), 28.2, 27.6, 26.4, 25.6, 25.5, 24.1 (CH_3, ar-CH), −5.4 (Al(CH_3)$_2$), −9.0 (Al(CH_3)$_2$) ppm. Anal. calcd for $C_{35}H_{53}N_3Al_2$ (569.789): C, 73.78; H, 9.38; N, 7.37. Found: C, 73.98; H, 9.67; N, 7.01.

Synthesis of (BDPPpyr-H)Y[(*μ*-Me)AlMe$_2$]$_2$ (6). In a glovebox, Y($AlMe_4$)$_3$ (**3c**) (180 mg, 0.51 mmol) was dissolved in 3 mL of hexane and added to a stirred solution of 1 equiv H_2BDPPpyr (H_2-[**1**]) (235 mg, 0.51 mmol) in 5 mL of hexane. Instant gas formation was observed. The reaction mixture was stirred another 24 h at ambient temperature while first the formation of a white precipitate was observed. After approximately 6 h, the white precipitate turned yellowish and partly redissolved. The product was separated by centrifugation and washed three times with 3 mL of hexane to yield **6** (256 mg, 0.37 mmol, 73%) as powdery yellow solid. Crystallization from hexane solution at −35 °C gave yellow crystals of **6** in good yields suitable for X-ray diffraction analysis. IR (Nujol, cm^{-1}): 1602 m, 1575 m, 1461 vs Nujol, 1379 vs Nujol, 1306 m, 1233 m, 1206 m, 1169 m, 1161 m, 1106 m, 1069 m, 1022 m, 969 w, 938 w, 895 w, 848 w, 806 w, 774 s, 721 s, 663 w, 627 w, 579 w, 569 w, 542 w. ^1H NMR (500 MHz, C_6D_6, 25 °C): *δ* = 7.23−6.93 (m, 6 H, ar), 6.74 (dd, $^3J \cong 7.2$ Hz, $^3J \cong 7.0$ Hz 1 H, pyr), 6.30 (d, $^3J \cong 7.0$ Hz, 1 H, pyr), 6.29 (d, $^3J \cong 7.2$ Hz, 1 H, pyr), 5.04 (d, $^2J \cong 17$ Hz, 1 H, N−CH_2), 4.82 (d, $^2J \cong 21$ Hz, 1 H, N−CH_2), 4.76 (d, $^2J \cong 21$ Hz, 1 H, N−CH_2), 4.06 (d, $^2J \cong 17$ Hz, 1 H, N−CH_2), 3.75 (sp, $^3J \cong 6.5$ Hz, 1 H, ar-CH), 3.71 (sp, $^3J \cong 6.5$ Hz, 1 H, ar-CH), 3.54 (sp, $^3J \cong 6.5$ Hz, 1 H, ar-CH), 3.24 (m, $^1J_{YH} \cong 14.0$ Hz, 1 H, ar-CH), 1.71 (dd, $^2J \cong 15.5$ Hz, $^3J \cong 8.0$ Hz, $^1J_{YH} \cong 15.5$ Hz, 1 H, Y−CH_2), 1.51 (d, $^3J \cong 6.5$ Hz, 3 H, ar-CH_3), 1.46 (d, $^3J \cong 6.5$ Hz, 3 H, ar-CH_3), 1.41 (d, $^3J \cong 6.5$ Hz, 6 H, ar-CH_3), 1.28 (d, $^3J \cong 6.5$ Hz, 3 H, ar-CH_3), 1.24 (d, $^3J \cong 6.5$ Hz, 3 H, ar-CH_3), 1.21 (d, $^3J \cong 6.5$ Hz, 3 H, ar-CH_3), 1.16 (dd, $^2J \cong 15.5$ Hz, $^3J \cong 3.5$ Hz, 1 H, Y−CH_2), −0.25 (s br, 9 H, Al(CH_3)$_3$), −0.71 (d, $^2J_{YH} \cong 1.2$ Hz, 9 H, Al(CH_3)$_3$) ppm. ^{13}C {^1H} NMR (126 MHz, C_6D_6, 25 °C): *δ* = 164.5, 160.2, 147.7, 147.1, 146.7, 146.5, 146.0, 142.6, 139.2, 125.6, 125.0, 124.5, 119.8, 118.4 (C_{ar}), 66.2, 65.5 (N−CH_2), 36.5 (d, $^1J_{YC} \cong 13.2$ Hz, Y-CH_2), 31.7, 30.0, 29.0, 28.7, 28.6, 28.2, 28.1, 27.7 (CH_3, ar-CH), −2.5 (s br, Al-(CH_3)$_3$) ppm. Anal. calcd for $C_{37}H_{58}N_3Al_2Y$ (687.756): C, 64.62; H, 8.50; N, 6.11. Found: C, 64.25; H, 8.65; N, 5.94.

Synthesis of (BDPPpyr-H)Lu[(*μ*-Me)AlMe$_2$](THF) (7) and [Lu(BDPPpyr-H)]$_2$ (8). To a stirred suspension of **4b** (102 mg, 0.14 mmol) in 3 mL of hexane 3 mL THF were added dropwise. The white solid dissolved immediately and the reaction mixture turned red. After stirring for 4 h at ambient temperature the solvent was removed in vacuo to form a yellow solid, which was washed three times with 2 mL of hexane and dried under vacuum to yield a powdery yellow solid. Crystallization from hexane solutions yielded two different batches of yellow single crystals. Low-yield product (and intermediate) **7** could be identified by X-ray structure analysis and NMR spectroscopy: ^1H NMR (600 MHz, C_6D_6, 25 °C): *δ* = 7.33−7.04 (m, 6 H, ar), 7.01 (d, $^3J \cong 7.8$ Hz, 1 H, pyr), 6.80 (dd, $^3J \cong 7.8$ Hz, 1 H, pyr), 6.41 (d, $^3J \cong 7.8$ Hz, 1 H, pyr), 5.50 (d, $^2J \cong 18.0$ Hz, 1 H, N−CH_2), 5.11 (d, $^2J \cong 21.0$ Hz, 1 H, N−CH_2), 4.82 (d, $^2J \cong 21.0$ Hz, 1 H, N−CH_2), 4.73 (d, $^2J \cong 18.0$ Hz, 1 H, N−CH_2), 4.31 (sp, $^3J \cong 6.6$ Hz, 1 H, ar-CH), 3.73 (sp, $^3J \cong 7.2$ Hz, 1 H, ar-CH), 3.55 (sp, $^3J \cong 6.6$ Hz, 1 H, ar-CH), 3.19 (m, 2 H, THF), 3.10 (m, 2 H, THF), 1.65 (d, $^3J \cong 6.6$ Hz, 3 H, ar-CH_3), 1.48 (d, $^3J \cong 6.6$ Hz, 3 H, ar-CH_3), 1.46 (d, $^3J \cong 6.6$ Hz, 3 H, ar-CH_3), 1.35 (d, $^3J \cong 6.6$ Hz, 3 H, ar-CH_3), 1.30 (d, $^3J \cong 7.2$ Hz, 3 H, ar-CH_3), 1.22 (m, 4 H, THF), 1.15 (d, $^3J \cong 7.2$ Hz, 3 H, ar-CH_3), 0.89 (s, 3 H, ar-CH_3), 0.87 (s, 3 H, ar-CH_3), −0.24 (s br, 9 H, Al(CH_3)$_3$) ppm. ^{13}C{^1H}NMR (151 MHz, C_6D_6, 25 °C): *δ* = 164.7, 164.0, 157.4, 152.5, 149.8, 147.3, 138.5, 126.7, 124.5, 123.9, 123.4, 122.9, 121.8, 118.6, 118.1 (C_{ar}), 95.2 (C_{quart}), 70.6 (THF), 68.0, 61.7 (N−CH_2), 31.9, 29.0, 28.3, 28.0, 26.4, 25.5, 24.1, 23.9, 23.0 (CH_3, ar-CH, THF), −1.0 (s br, Al(CH_3)$_3$) ppm. Complex **8** is the thermodynamically favored and preferred crystallization product obtainable in high crystallized yield (128 mg, 0.10 mmol, 74%). IR (Nujol, cm^{-1}): 1613 m, 1577 m, 1458 vs Nujol, 1380 vs

Nujol, 1313 m, 1256 m, 1209 m, 1194 m, 1163 m, 1121 m, 1095 w, 1059 m, 1018 w, 976 m, 940 w, 899 w, 862 w, 811 w, 774 s, 728 s, 629 w, 552 w. ^{1}H NMR (600 MHz, C_6D_6, 25 °C): δ = 7.33−6.99 (m, 12 H, ar), 6.83 (dd, $^3J \cong$ 7.8 Hz, 2 H, pyr), 6.73 (d, $^3J \cong$ 7.8 Hz, 2 H, pyr), 6.64 (d, $^3J \cong$ 7.8 Hz, 2 H, pyr), 5.70 (d, $^2J \cong$ 18.0 Hz, 2 H, N−CH_2), 5.04 (d, $^2J \cong$ 19.8 Hz, 2 H, N−CH_2), 4.62 (d, $^2J \cong$ 18.0 Hz, 2 H, N−CH_2), 4.23 (d, $^2J \cong$ 19.8 Hz, 2 H, N−CH_2), 3.76 (sp, $^3J \cong$ 7.2 Hz, 2 H, ar-CH), 3.68 (sp, $^3J \cong$ 6.6 Hz, 2 H, ar-CH), 3.11 (sp, $^3J \cong$ 6.6 Hz, 2 H, ar-CH), 1.52 (d, $^3J \cong$ 7.2 Hz, 6 H, ar-CH_3), 1.47 (d, $^3J \cong$ 6.6 Hz, 6 H, ar-CH_3), 1.42 (d, $^3J \cong$ 6.6 Hz, 6 H, ar-CH_3), 1.36 (s, 6 H, ar-CH_3), 1.24 (s, 6 H, ar-CH_3), 1.07 (d, $^3J \cong$ 6.6 Hz, 6 H, ar-CH_3), 0.96 (d, $^3J \cong$ 6.6 Hz, 6 H, ar-CH_3), 0.95 (d, $^3J \cong$ 7.2 Hz, 6 H, ar-CH_3) ppm. ^{13}C {^{1}H} NMR (151 MHz, C_6D_6, 25 °C): δ = 164.6, 164.0, 157.4, 152.5, 149.8, 147.3, 138.4, 126.6, 124.5, 123.9, 123.5, 122.7, 121.6, 118.7, 118.2 (C_{ar}), 95.1 (C_{quart}), 66.2, 65.1 (N−CH_2), 31.9, 29.7, 28.0, 27.2, 26.8, 25.4, 23.8, 23.0 (CH_3, ar-CH) ppm. Anal. calcd for $C_{60}H_{80}N_6Lu_2$ (1235.275): C, 58.34; H, 6.53; N, 6.80. Found: C, 58.23; H, 6.19; N, 6.64.

Single-Crystal X-Ray Structures. Crystal data and details of the structure determination are presented in Table 7. The crystals were placed in a nylon loop containing Paratone oil (Hampton Research) and mounted directly into the N_2 cold stream (Oxford Cryosystems Series 700) on a Bruker AXS SMART 2K CCD diffractometer. Data were collected by means of 0.3° ω-scans in four orthogonal φ-settings using Mo K_α radiation (λ = 0.71073 Å). Data collection was controlled using the program SMART, data integration using SAINT, and structure solution and model refinement using SHELXS-97 and SHELXL-97,[64] respectively.[65] Non-coordinating methyl groups were refined as rigid and rotating (difference Fourier density optimization) CH_3 groups around the respective Al−C bonds. Coordinating methyl groups were refined as rigid pyramidal groups with the same C−H and H−H distances as for the previous, but with the threefold axis of the pyramidal rigid group allowed to be nonparallel with the C−Al bond axis. The isotropic displacement parameters for all methyl H-atoms were set to be 1.5 times that of the pivot C-atom.

Acknowledgment. Financial support from the Norwegian Research Council and the program Nanoscience@UiB is gratefully acknowledged.

Supporting Information Available: CCDC 651955−651958 and CCDC 652609 contain the supplementary crystallographic data for this paper. Copies of the data can be obtained free of charge from The Cambridge Crystallographic Data Centre, via www.ccdc.cam.ac.uk/data_request/cif. This material is available free of charge via the Internet at http://pubs.acs.org.

OM700830K

(64) Sheldrick, G. M. *SHELXL-97*, University of Göttingen: Göttingen, Germany, 1998.

(65) (a) *SMART*, version 5.054; Bruker AXS Inc.: Madison, WI, 1999; *SAINT*, version 6.45a; Bruker AXS Inc.: Madison, WI, 2001. (b) Sheldrick, G. M. *SHELXS-97*; University of Göttingen: Göttingen, Germany, 2003.